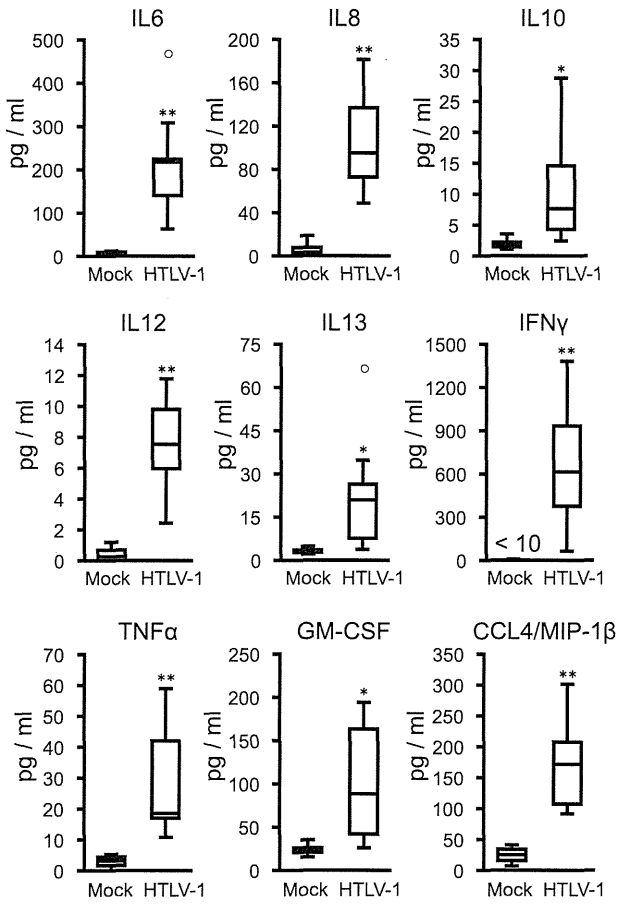

Figure 4. Induction of inflammatory cytokines in infected IBMI-huNOG mice. Human cytokine concentrations in plasma. Plasma was collected following sacrifice of mock-infected (n = 4) and HTLV-1–infected mice (n = 8). Seventeen cytokines were quantified using a cytokine bead array system. The concentrations of human IL-6, IL-8, IL-10, IL-12, IL-13, IFNγ, TNF-α, GM-CSF, and CCL4/MIP-1β are shown, all of which were significantly increased in the plasma of HTLV-1–infected mice. Increased expressions of the other 6 cytokines (IL-2, IL-4, IL-7, IL-17, G-CSF, and MCP-1) were also observed in infected mice but not statistically significant. On the other hand, little decrease in the concentrations of IL-1 and IL-5 was seen. Asterisks in each panel represent significant differences vs mock-infected mice (*$P < .05$, **$P < .01$ by Mann-Whitney U test).

human stem cells directly into the bone marrow cavity of NOD/Shi-SCID/IL-2Rγc null (NOG) mice using an IBMI method.

The efficacy of humanization achieved in this model is markedly superior to other procedures, such as intrahepatic or intravenous injection of human hematopoietic stem cells.[21,22,29] While T-lineage–cell populations become dominant over B-cell populations in the lymphoid organs of other humanized mouse systems within a few months after transplantation, in IBMI-huNOG mice the B-to-T-cell ratio remained constant for >8 months posttransplantation (Figure 1E). One possible explanation for this difference is that direct injection of hematopoietic stem cell preparations into the bone marrow of recipient mice improves the colonization efficiency of long-term stem cells.[27,46] Moreover, we used $CD133^+$ cells to generate IBMI-huNOG mice. CD133, the early hematopoietic progenitor cell marker, is thought to be ancestral to CD34 in human hematopoiesis.[47] Previous studies have revealed that $CD133^+$ cells were capable of differentiating not only into hematopoietic cells but also into endothelial, stromal, neuronal, and other type of cells.[47-49] It is possible that human mesenchymal stromal cells derived from $CD133^+$ cells support the development and maintenance of human B cells in the bone marrow microenvironment.

Having established a new humanized mouse model, we then infected IBMI-huNOG mice with HTLV-1 through inoculation with sublethally irradiated HTLV-1–producing cells.[28] HTLV-1–infected IBMI-huNOG mice recapitulated a large number of pathological features characteristic of ATL patients, including hyperproliferation of $CD3^+$ T cells, clonal proliferation of $CD25^+$ CD4 T cells, the appearance of flower cells in the periphery, hepatosplenomegaly, inflammatory hypercytokinemia, and down-regulation of CD3 on T cells.

Overgrowth of infected T cells was correlated with the expression of CD25 on CD4 T cells, consistent with recent reports.[17] However, the substantial proportion of $CD25^-$ CD4 T cells were also infected and identical T-cell clones, as determined by provirus integration site, were detected as the most abundant clones in both $CD25^-$ and $CD25^+$ CD4 T-cell populations, suggesting that CD25 expression likely occurs after infection in the course of clonal expansion. In addition, the expressions of *tax* and CD25 were inversely correlated. Further research will be necessary to identify molecular events associated with the suppression of *tax* expression in HTLV-1–infected $CD25^+$ CD4 T cells in relation to the development of ATL.

Banerjee et al[16] described the development of T-cell lymphoma following bone marrow transplantation of HTLV-1–infected $CD34^+/CD38^-$ hematopoietic stem cells into a NOD/SCID mouse. The lymphoma cells in these mice were capable of infiltrating into multiple organs but represented only $CD25^-$ or $CD25^{low}$ phenotypes. In contrast, HTLV-1–infected IBMI-huNOG mice developed leukemia in $CD25^+$ CD4 T cells, similar to that observed in ATL patients. The mechanism underlying this difference is unknown but may be due to differences in the developmental stage of T cells at the time of infection. Indeed, HTLV-1 infection in a different humanized mouse model, generated by intrahepatic transplantation of human $CD34^+$ stem cells into $Rag2^{-/-}\gamma c^{-/-}$ mice, induced formation of thymomas/lymphomas in mature CD4 T cells.[17] In this case, HTLV-1 infection was carried out 4 and 8 weeks after transplantation of $CD34^+$ hematopoietic stem cells, giving the human immune system time to develop. Thus the infection of $CD34^+$ stem cells per se does not appear to be sufficient for the induction of mature $CD25^+$ T cell malignancies and may require more developed lymphoid cells or a more appropriate microenvironment capable of supporting cell development.

Furthermore, HTLV-1–infected IBMI-huNOG mice almost exclusively developed leukemia, whereas HTLV-1 infection in the other humanized mouse models described above preferentially induced formation of lymphoma or thymoma. The reason for this difference is not clear but may stem from differences in the timing of T-cell infection. IBMI-huNOG mice were infected after the human hematopoietic system had been fully established, while in the other systems the infection was carried out before or shortly after stem cell transplantation.

In addition to leukemic growth of $CD25^+$ T cells, we also observed formation of flower cells in the peripheral blood of infected mice at later time points postinfection (>16 wpi). Although transformed T cells derived from Tax-transgenic mice were found to exhibit similar morphology,[15] none of the animal models described so far had recapitulated this pathology. Clonal analysis performed as part of this study demonstrated that the expansion of $CD25^+$ T-cell clones preceded the appearance of flower cells in periphery, suggesting a sequence of events that occurs during development of the malignancy. Thus, chronological

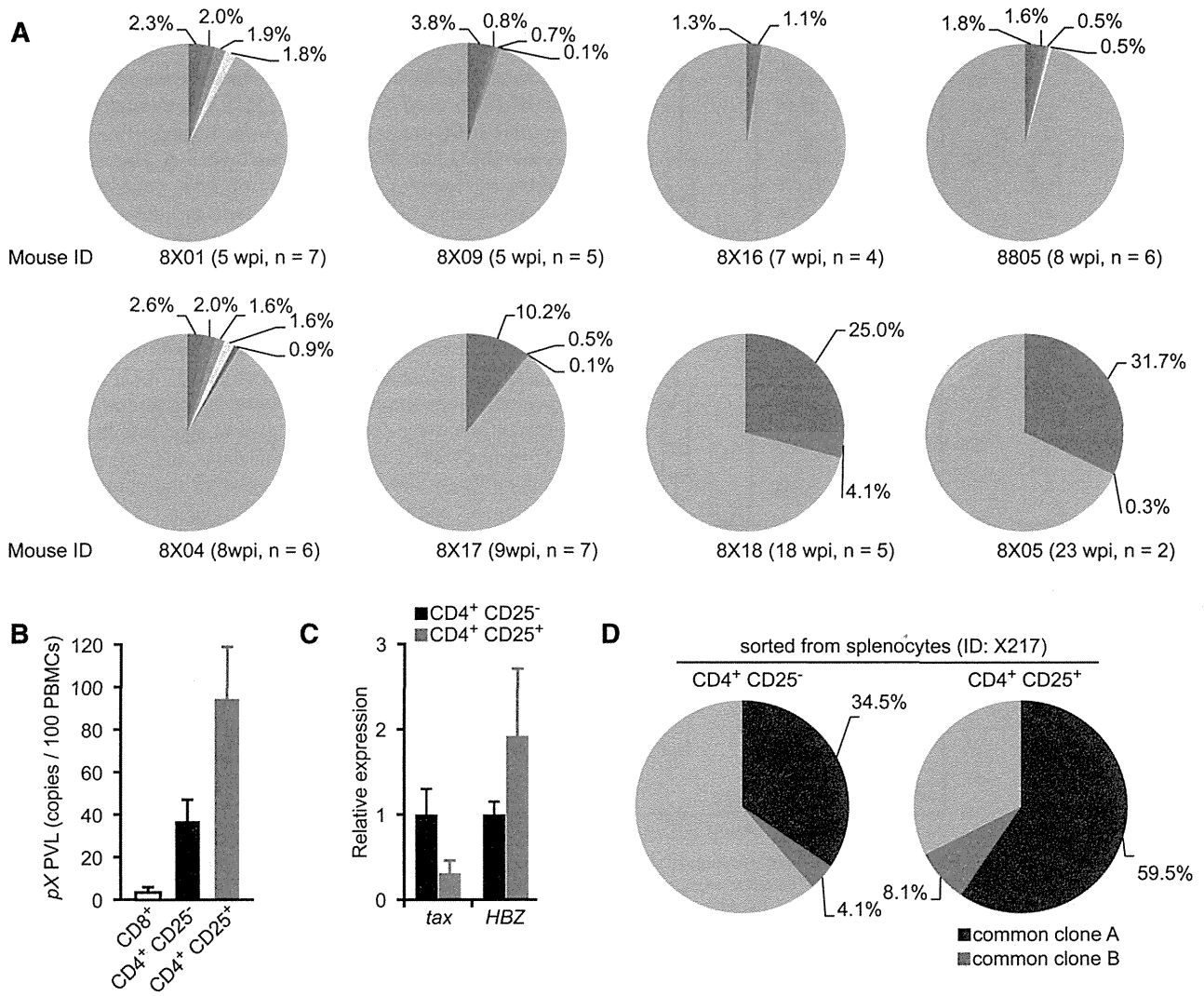

Figure 5. Progression of clonality in splenocytes of infected IBMI-huNOG. (A) Occupancy of HTLV-1–infected clones in the spleen. Abundant integration sites of HTLV-1 provirus were amplified by IL-PCR and subcloned into plasmids. The number of integration sites in each splenic DNA sample was determined by quantitative PCR using the clone-specific nucleotide sequence for each integration site. Results from 8 individual HTLV-1–infected mice are shown as pie charts. Size of the slice is proportional to the relative abundance of T-cell clones successfully amplified by IL-PCR, while data of minor clones with less than 0.1% occupancy were omitted. Gray regions represent clones with undefined integration sites. n, number of integration sites determined by nucleotide sequence of cloned PCR fragments in each mouse. (B) PVLs of specifiedT-cell populations. Splenocytes from HTLV-1–infected mice (n = 5) were sorted into $CD25^-$ or $CD25^+$ CD4 T cells and $CD8^+$ T cells. Genomic DNA isolated from each T-cell population was analyzed for PVL by real-time PCR using primers for the *pX* region of HTLV-1. (C) Comparative analysis of viral transcripts in $CD25^-$ and $CD25^+$ CD4 T-cell populations. Splenocytes from HTLV-1–infected mice (n = 5) are identical to those in mentioned above. The expression levels of *tax* (left) and *HBZ* (right) were analyzed by quantitative RT-PCR and were normalized to that of *HPRT1*. Results are presented as the fold change compared with the value in $CD25^-$ CD4 T cells. (D) Detection of common T-cell clones in the $CD25^-$ and $CD25^+$ CD4 T-cell populations. Clonal occupancy in both $CD25^-$ and $CD25^+$ populations are presented as pie charts. Two abundant common clones were analyzed for occupancy. Identified integration sites are listed in supplemental Table 5. The purity of each sorted population was >95% (supplemental Figure 3).

analysis of genetic and/or biochemical events in infected T cells from this mouse model should provide substantial information regarding the development of ATL.

We detected HLA-restricted CTLs against Tax protein of HTLV-1, as demonstrated in the peripheral blood of HTLV-1–infected carriers,[43] confirming the presence of an acquired immune response. Furthermore, the frequency of CTLs in CD8 T-cell populations were inversely correlated with the number of infected T cells in the spleen of humanized mice, similar to observations in HTLV-1–infected individuals.[43] The presence of functional T cells was also supported by the production of IgG antibodies specific to HTLV-1. Although humanized mice established by the transplantation of $CD34^+$ hematopoietic stem cells have been reported to produce antibodies against specific pathogens such as EBV,[22] HIV-1,[21] and DENV,[50] class switching from IgM to IgG was observed in only a few cases, likely due to immature T-cell development. In the IBMI-huNOG system, however, IgG production against HTLV-1 structural protein was observed after biphasic induction of antibodies after 8 weeks, indicating a functional interaction between CD4 T cells and B cells specific for viral antigens. Taken together, these data demonstrate induction of an adaptive immune response against HTLV-1 in HTLV-1–infected IBMI-huNOG mice, which may play an important role as selective pressure in the expansion of malignant T-cell clones.

In conclusion, our study demonstrates that the HTLV-1–infected IBMI-huNOG mouse represents a novel model that will facilitate elucidation of the molecular mechanism of in vivo development of ATL. Moreover, our model can also be used to develop and evaluate

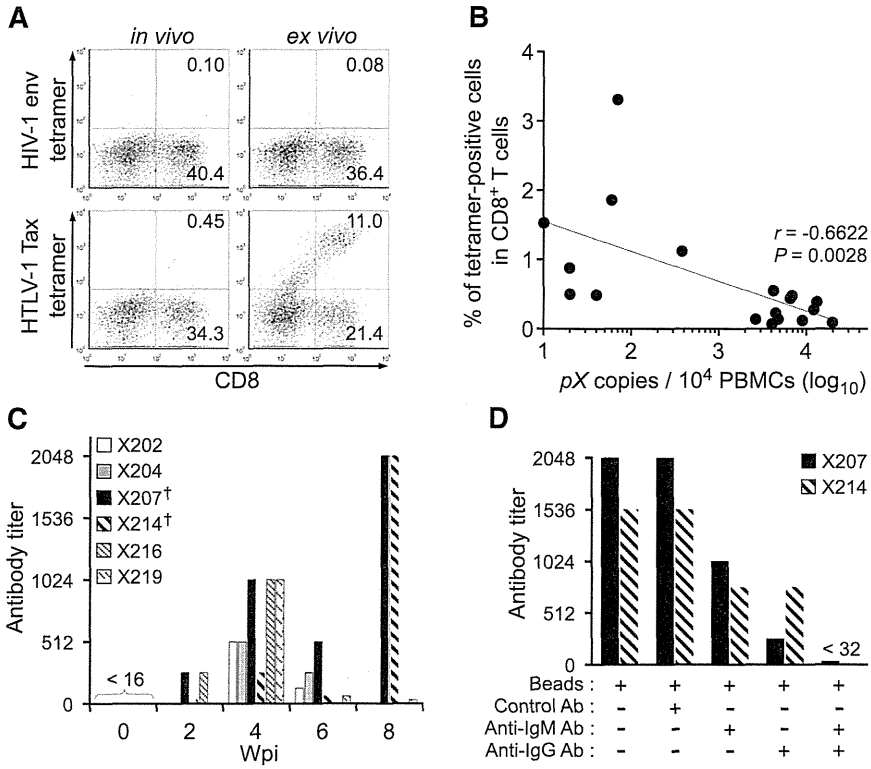

Figure 6. Induction of cellular and humoral immune responses against HTLV-1 in infected IBMI-huNOG mice. (A) Detection of HTLV-1–specific HLA-A*24:02-restricted CTLs. Splenocytes from HTLV-1–infected mice at 8 wpi were stained with human CD8 and Tax301-309 tetramer or HIV-1 env gp160 tetramer as a negative control, respectively. Representative results of tetramer-positive CD8 T cells in vivo (left) and ex vivo culture with Tax peptide (right) are shown. (B) Inverse correlation between PVL and the frequency of Tax301-309–specific CTLs. The percentages of tetramer-positive CD8 T cells and PVL in the spleens of 18 HTLV-1–infected mice are shown. One dot represents the result of an individual HTLV-1–infected mouse. Spearman's rank-correlation coefficient (r^2) was used to identify statistically significant correlations. (C) HTLV-1–specific antibody responses in HTLV-1–infected mice. HTLV-1–specific antibody titers in plasma were monitored by the particle agglutination method. Each bar represents an individual mouse. The plasma of indicated mice prior to infection were used as negative-controls (shown as 0 wpi), and these titers were undetectable level (<16). Mice with daggers (mouse ID: X207 and X214) showed biphasic induction of antibody responses; titers peaked at 8 wpi. (D) Detection of HTLV-1–specific IgM or IgG antibody. Antibody depletion was performed by addition of goat antibodies against human IgG or IgM and anti-goat antibody conjugated magnetic beads to the plasma of two mice, as shown in panel C (indicated by daggers). Bars represent antibody titers in the individual X207 and X214 mice. Ab, antibody.

novel preclinical therapies that target viral gene products or cellular molecules critical for viral replication as well as evaluate the efficacy of vaccine candidates to prevent viral expansion in vivo.

Acknowledgments

The authors thank Drs R. Tatsumi and Y. Adachi for advice in establishing humanized mice and assistance with the pathological analysis, respectively. The authors are grateful to the Japanese Red Cross Kinki Cord Blood Bank for providing the samples used in this study.

This work was supported by Grants-in-Aid for Scientific Research C from the Ministry of Education, Culture, Sports, Science and Technology of Japan (grants 21590515 and 24590562) (J.F.); a MEXT-Supported Program for the Strategic Research Foundation at Private Universities; and Health and Labour Sciences Research Grants for Research on Emerging and Re-emerging Infectious Diseases from Ministry of Health, Labour and Welfare (grant 24171601) (T.U.) (grant 23211801) (M. Tanaka).

Authorship

Contribution: K.T. and J.F. designed the research; K.T. and R.X. established and maintained humanized mice; K.T., R.X., M. Tei and T.U. carried out experiments; M. Tanaka was involved in the IL-PCR analysis; K.T., R.X., M. Tei, and J.F. analyzed results; N.T. performed statistical analysis; K.T. designed the figures; and K.T. and J.F. wrote the paper.

Conflict-of-interest disclosure: The authors declare no competing financial interests.

Correspondence: Jun-ichi Fujisawa, Department of Microbiology, Kansai Medical University, 2-5-1 Shin-machi, Hirakata, Osaka 573-1010, Japan; e-mail: fujisawa@hirakata.kmu.ac.jp.

References

1. Hinuma Y, Nagata K, Hanaoka M, et al. Adult T-cell leukemia: antigen in an ATL cell line and detection of antibodies to the antigen in human sera. *Proc Natl Acad Sci USA.* 1981;78(10):6476-6480.
2. Poiesz BJ, Ruscetti FW, Gazdar AF, Bunn PA, Minna JD, Gallo RC. Detection and isolation of type C retrovirus particles from fresh and cultured lymphocytes of a patient with cutaneous T-cell lymphoma. *Proc Natl Acad Sci USA.* 1980;77(12):7415-7419.
3. Osame M, Usuku K, Izumo S, et al. HTLV-I associated myelopathy, a new clinical entity. *Lancet.* 1986;1(8488):1031-1032.
4. Kondo T, Kono H, Miyamoto N, et al. Age- and sex-specific cumulative rate and risk of ATLL for HTLV-I carriers. *Int J Cancer.* 1989;43(6):1061-1064.
5. Boxus M, Twizere JC, Legros S, Dewulf JF, Kettmann R, Willems L. The HTLV-1 Tax interactome. *Retrovirology.* 2008;5:76.
6. Matsuoka M, Jeang KT. Human T-cell leukemia virus type 1 (HTLV-1) and leukemic transformation: viral infectivity, Tax, HBZ and therapy. *Oncogene.* 2011;30(12):1379-1389.
7. Yoshida M, Seiki M, Yamaguchi K, Takatsuki K. Monoclonal integration of human T-cell leukemia provirus in all primary tumors of adult T-cell leukemia suggests causative role of human T-cell leukemia virus in the disease. *Proc Natl Acad Sci USA.* 1984;81(8):2534-2537.
8. Shimoyama M, Minato K, Tobinai K, et al. Atypical adult T-cell leukemia-lymphoma: diverse clinical manifestations of adult T-cell leukemia-lymphoma. *Jpn J Clin Oncol.* 1983;13(Suppl 2):165-187.
9. Okayama A, Tachibana N, Ishihara S, et al. Increased expression of interleukin-2 receptor alpha on peripheral blood mononuclear cells in HTLV-I tax/rex mRNA-positive asymptomatic carriers. *J Acquir Immune Defic Syndr Hum Retrovirol.* 1997;15(1):70-75.

10. Bieberich CJ, King CM, Tinkle BT, Jay G. A transgenic model of transactivation by the Tax protein of HTLV-I. *Virology.* 1993;196(1):309-318.
11. Feuer G, Zack JA, Harrington WJ Jr, et al. Establishment of human T-cell leukemia virus type I T-cell lymphomas in severe combined immunodeficient mice. *Blood.* 1993;82(3): 722-731.
12. Kondo A, Imada K, Hattori T, et al. A model of in vivo cell proliferation of adult T-cell leukemia. *Blood.* 1993;82(8):2501-2509.
13. Furuta RA, Sugiura K, Kawakita S, Inada T, Ikehara S, Matsuda T, Fujisawa J. Mouse model for the equilibration interaction between the host immune system and human T-cell leukemia virus type 1 gene expression. *J Virol.* 2002;76(6): 2703-2713.
14. Dewan MZ, Terashima K, Taruishi M, et al. Rapid tumor formation of human T-cell leukemia virus type 1-infected cell lines in novel NOD-SCID/ gammac(null) mice: suppression by an inhibitor against NF-kappaB. *J Virol.* 2003;77(9): 5286-5294.
15. Hasegawa H, Sawa H, Lewis MJ, et al. Thymus-derived leukemia-lymphoma in mice transgenic for the Tax gene of human T-lymphotropic virus type I. *Nat Med.* 2006;12(4):466-472.
16. Banerjee P, Tripp A, Lairmore MD, et al. Adult T-cell leukemia/lymphoma development in HTLV-1-infected humanized SCID mice. *Blood.* 2010;115(13):2640-2648.
17. Villaudy J, Wencker M, Gadot N, et al. HTLV-1 propels thymic human T cell development in "human immune system" Rag2$^{-/-}$ gamma c$^{-/-}$ mice. *PLoS Pathog.* 2011;7(9):e1002231.
18. Satou Y, Yasunaga J, Zhao T, et al. HTLV-1 bZIP factor induces T-cell lymphoma and systemic inflammation in vivo. *PLoS Pathog.* 2011;7(2): e1001274.
19. Kazanji M. HTLV type 1 infection in squirrel monkeys (Saimiri sciureus): a promising animal model for HTLV type 1 human infection. *AIDS Res Hum Retroviruses.* 2000;16(16):1741-1746.
20. Lairmore MD, Silverman L, Ratner L. Animal models for human T-lymphotropic virus type 1 (HTLV-1) infection and transformation. *Oncogene.* 2005;24(39):6005-6015.
21. Watanabe S, Terashima K, Ohta S, et al. Hematopoietic stem cell-engrafted NOD/SCID/ IL2Rgamma null mice develop human lymphoid systems and induce long-lasting HIV-1 infection with specific humoral immune responses. *Blood.* 2007;109(1):212-218.
22. Yajima M, Imadome K, Nakagawa A, et al. A new humanized mouse model of Epstein-Barr virus infection that reproduces persistent infection, lymphoproliferative disorder, and cell-mediated and humoral immune responses. *J Infect Dis.* 2008;198(5):673-682.
23. Hasegawa A, Ohashi T, Hanabuchi S, Kato H, Takemura F, Masuda T, Kannagi M. Expansion of human T-cell leukemia virus type 1 (HTLV-1) reservoir in orally infected rats: inverse correlation with HTLV-1-specific cellular immune response. *J Virol.* 2003;77(5):2956-2963.
24. Kannagi M, Hasegawa A, Kinpara S, Shimizu Y, Takamori A, Utsunomiya A. Double control systems for human T-cell leukemia virus type 1 by innate and acquired immunity. *Cancer Sci.* 2011; 102(4):670-676.
25. Ito M, Hiramatsu H, Kobayashi K, et al. NOD/SCID/gamma(c)(null) mouse: an excellent recipient mouse model for engraftment of human cells. *Blood.* 2002;100(9):3175-3182.
26. Kushida T, Inaba M, Hisha H, et al. Intra-bone marrow injection of allogeneic bone marrow cells: a powerful new strategy for treatment of intractable autoimmune diseases in MRL/lpr mice. *Blood.* 2001;97(10):3292-3299.
27. Wang J, Kimura T, Asada R, et al. SCID-repopulating cell activity of human cord blood-derived CD34- cells assured by intra-bone marrow injection. *Blood.* 2003;101(8):2924-2931.
28. Miyoshi I, Kubonishi I, Yoshimoto S, et al. Type C virus particles in a cord T-cell line derived by co-cultivating normal human cord leukocytes and human leukaemic T cells. *Nature.* 1981; 294(5843):770-771.
29. Nie C, Sato K, Misawa N, et al. Selective infection of CD4+ effector memory T lymphocytes leads to preferential depletion of memory T lymphocytes in R5 HIV-1-infected humanized NOD/SCID/IL-2Rgammanull mice. *Virology.* 2009;394(1):64-72.
30. Takamori A, Hasegawa A, Utsunomiya A, et al. Functional impairment of Tax-specific but not cytomegalovirus-specific CD8+ T lymphocytes in a minor population of asymptomatic human T-cell leukemia virus type 1-carriers. *Retrovirology.* 2011;8:100.
31. Ueno S, Umeki K, Takajo I, et al. Proviral loads of human T-lymphotropic virus Type 1 in asymptomatic carriers with different infection routes. *Int J Cancer.* 2012;130(10):2318-2326.
32. Etoh K, Tamiya S, Yamaguchi K, et al. Persistent clonal proliferation of human T-lymphotropic virus type I-infected cells in vivo. *Cancer Res.* 1997; 57(21):4862-4867.
33. Umeki K, Hisada M, Maloney EM, Hanchard B, Okayama A. Proviral loads and clonal expansion of HTLV-1-infected cells following vertical transmission: a 10-year follow-up of children in Jamaica. *Intervirology.* 2009;52(3):115-122.
34. Hiramatsu H, Nishikomori R, Heike T, Ito M, Kobayashi K, Katamura K, Nakahata T. Complete reconstitution of human lymphocytes from cord blood CD34+ cells using the NOD/SCID/ gammacnull mice model. *Blood.* 2003;102(3): 873-880.
35. Nitta T, Tanaka M, Sun B, Hanai S, Miwa M. The genetic background as a determinant of human T-cell leukemia virus type 1 proviral load. *Biochem Biophys Res Commun.* 2003;309(1):161-165.
36. Yamano Y, Araya N, Sato T, et al. Abnormally high levels of virus-infected IFN-gamma+ CCR4+ CD4+ CD25+ T cells in a retrovirus-associated neuroinflammatory disorder. *PLoS ONE.* 2009;4(8):e6517.
37. Matsuda M, Maeda Y, Shirakawa C, et al. CD3 down-regulating factor in sera and culture supernatants of leukaemic cells from patients with adult T cell leukaemia. *Br J Haematol.* 1993;83(2): 212-217.
38. Yamada Y, Ohmoto Y, Hata T, et al. Features of the cytokines secreted by adult T cell leukemia (ATL) cells. *Leuk Lymphoma.* 1996;21(5-6): 443-447.
39. Chiba K, Hashino S, Izumiyama K, Toyoshima N, Suzuki S, Kurosawa M, Asaka M. Multiple osteolytic bone lesions with high serum levels of interleukin-6 and CCL chemokines in a patient with adult T cell leukemia. *Int J Lab Hematol.* 2009;31(3):368-371.
40. Chen J, Petrus M, Bryant BR, et al. Autocrine/ paracrine cytokine stimulation of leukemic cell proliferation in smoldering and chronic adult T-cell leukemia. *Blood.* 2010;116(26):5948-5956.
41. Ohshima K, Mukai Y, Shiraki H, Suzumiya J, Tashiro K, Kikuchi M. Clonal integration and expression of human T-cell lymphotropic virus type I in carriers detected by polymerase chain reaction and inverse PCR. *Am J Hematol.* 1997; 54(4):306-312.
42. Kurihara K, Harashima N, Hanabuchi S, et al. Potential immunogenicity of adult T cell leukemia cells in vivo. *Int J Cancer.* 2005;114(2):257-267.
43. Akimoto M, Kozako T, Sawada T, et al. Anti-HTLV-1 tax antibody and tax-specific cytotoxic T lymphocyte are associated with a reduction in HTLV-1 proviral load in asymptomatic carriers. *J Med Virol.* 2007;79(7):977-986.
44. Harashima N, Kurihara K, Utsunomiya A, et al. Graft-versus-Tax response in adult T-cell leukemia patients after hematopoietic stem cell transplantation. *Cancer Res.* 2004;64(1):391-399.
45. Kozako T, Arima N, Toji S, et al. Reduced frequency, diversity, and function of human T cell leukemia virus type 1-specific CD8+ T cell in adult T cell leukemia patients. *J Immunol.* 2006; 177(8):5718-5726.
46. Nakamura K, Inaba M, Sugiura K, Yoshimura T, Kwon AH, Kamiyama Y, Ikehara S. Enhancement of allogeneic hematopoietic stem cell engraftment and prevention of GVHD by intra-bone marrow bone marrow transplantation plus donor lymphocyte infusion. *Stem Cells.* 2004; 22(2):125-134.
47. Jaatinen T, Hemmoranta H, Hautaniemi S, et al. Global gene expression profile of human cord blood-derived CD133+ cells. *Stem Cells.* 2006; 24(3):631-641.
48. Herrera MB, Bruno S, Buttiglieri S, et al. Isolation and characterization of a stem cell population from adult human liver. *Stem Cells.* 2006;24(12): 2840-2850.
49. Martin-Rendon E, Hale SJ, Ryan D, et al. Transcriptional profiling of human cord blood CD133+ and cultured bone marrow mesenchymal stem cells in response to hypoxia. *Stem Cells.* 2007;25(4):1003-1012.
50. Kuruvilla JG, Troyer RM, Devi S, Akkina R. Dengue virus infection and immune response in humanized RAG2($^{-/-}$)gamma(c)($^{-/-}$) (RAG-hu) mice. *Virology.* 2007;369(1):143-152.

blood 2014 123: 346-355
doi:10.1182/blood-2013-06-508861 originally published online November 6, 2013

An animal model of adult T-cell leukemia: humanized mice with HTLV-1–specific immunity

Kenta Tezuka, Runze Xun, Mami Tei, Takaharu Ueno, Masakazu Tanaka, Norihiro Takenouchi and Jun-ichi Fujisawa

Blood (print ISSN 0006-4971, online ISSN 1528-0020), is published weekly by the American Society of Hematology, 2021 L St, NW, Suite 900, Washington DC 20036.

INTERNAL MEDICINE

□ CASE REPORT □

Human T-lymphotropic Virus Type-I (HTLV-I)-associated Myelopathy with Bulbar Palsy-type Amyotrophic Lateral Sclerosis-like Symptoms

Rina Ando, Noriko Nishikawa, Tomoaki Tsujii, Hirotaka Iwaki, Hayato Yabe, Masahiro Nagai and Masahiro Nomoto

Abstract

We herein report a case of Human T-lymphotropic virus type-I (HTLV-I)-associated myelopathy with bulbar palsy-type amyotrophic lateral sclerosis-like symptoms. A 52-year-old woman developed dyslalia at approximately 40 years of age, which slowly progressed. She presented with muscular atrophy and increased tendon reflexes of the extremities as well as bulbar palsy, from which motor neuron disease was suspected. Cerebrospinal fluid (CSF) testing revealed no abnormalities except for an elevated neopterin concentration at 143.17 pmol/mL (normal ≤30 pmol/mL). Her serum and CSF anti-HTLV-I antibody titers were also high. Intravenous infusions of methylprednisolone decreased the CSF neopterin concentration to 50.33 pmol/mL. Subsequent oral prednisolone therapy was effective in alleviating the symptoms.

Key words: HTLV-I-associated myelopathy (HAM), bulbar palsy, amyotrophic lateral sclerosis (ALS), neopterin, anti-HTLV-I antibody, steroid therapy

(Intern Med 54: 1105-1107, 2015)
(DOI: 10.2169/internalmedicine.54.3660)

Introduction

Human T-lymphotropic virus type-I (HTLV-I)-associated myelopathy (HAM) is a slowly progressive myelopathy caused by one of the human retroviruses, HTLV-I. The principal clinical manifestations of HAM are spastic paraplegia and pollakiuria (1). Cerebrospinal fluid (CSF) testing in HAM patients shows high levels of anti-HTLV-I antibody titer and neopterin (2). Immunotherapies including steroids and interferon-alpha are applied for the treatment of HAM. We herein report a case of HAM with bulbar palsy, muscular atrophy, and weakness of the upper limbs and trunk that required differentiation from bulbar palsy-type amyotrophic lateral sclerosis (ALS).

Case Report

A 52-year-old woman presented with the main complaint of dyslalia and gait disturbance. She had no remarkable medical history and did not smoke or drink alcohol. Her mother had suffered from dyslalia that developed in her 40s and she died at 70 years of age.

The patient developed dyslalia at approximately 40 years of age, which slowly progressed. Aspiration occurred at approximately 50 years of age. She visited our clinic due to frequent falls on level ground. She presented with muscular atrophy and increased tendon reflexes of the extremities as well as bulbar palsy. Because her deceased mother reportedly had similar symptoms, familial ALS was suspected and she was admitted to hospital for further evaluation.

On admission, the patient's height was 161 cm and body weight was 38.6 kg. Her vital signs were normal. She was alert and had normal cognitive function. The patient's facial muscle strength was slightly reduced in the upper part and moderately reduced in the lower part. She also had symptoms of cranial nerve disorder which included constant mouth opening, forced crying, dysphagia, dyslalia, a loss of gag reflex, tongue atrophy, fasciculation, and poor tongue protrusion. There were no other abnormal symptoms in the

Department of Neurology and Clinical Pharmacology, Ehime University Graduate School of Medicine, Japan
Received for publication July 11, 2014; Accepted for publication September 18, 2014
Correspondence to Dr. Masahiro Nagai, mnagai@m.ehime-u.ac.jp

Table. **Cases of HAM Showing ALS-like Signs in the Literature**

	Matsuzaki et al.[4] (n=5)	Vernant et al.[7] (n=4)	Kuroda & Sugihara[5] (n=1)	Arimura et al.[6] (n=1)
Age at onset (years)	Mean: 52.2	49–77	57	67
Course (years)	Time to abasia: Mean:5	NR	Time to death: 4.5 years	NR
Bulbar palsy	2/5	2/4	+	+
Fasciculation in tongue	3/5	NR	+	NR
Muscular atrophy in extremities	5/5	4/4	+	+
Hyperreflexia	5/5	4/4	+	+
Babinski index	4/5	NR	+	NR
Sensory disturbance	4/5	0/4	–	+
Autonomic disturbance	4/5	1/4	+/–	+
Anti-HTLV-I antibody in CSF	5/5	NR	+	NR
Anti-HTLV-I antibody in serum	5/5	4/4	+	+
Effect of steroid therapy	Improved in 2/3 treated patients	NR	NR	NR

Abbreviations: ALS: amyotrophic lateral sclerosis, CSF: cerebrospinal fluid, HAM: HTLV-I-associated myelopathy, HTLV-I: Human T-lymphotropic virus type-I, NR: not reported

cranial nerve system. Her extremities were spastic, and systemic muscular atrophy and fasciculation were observed. A manual muscle test revealed muscle weakness, predominantly in the proximal muscles, and was graded a 4 out of 5. The jaw reflex and tendon reflexes of the extremities were hyperactive. Babinski reflex was bilaterally positive and the patient had a spastic gait. Her autonomic symptoms included constipation and micturition frequency at approximately 8 to 10 times daily. She had no coordination disturbance or sensory disturbance.

Blood tests showed no significantly abnormal values in the patient's blood cell counts, blood biochemistry, markers of the auto-immune system, or various tumor markers. General CSF testing revealed no abnormal results. Magnetic resonance imaging scans of the brain and spinal cord revealed no abnormal findings. Nerve conduction studies also showed normal results. Needle electromyography showed acute neurogenic changes in the first dorsal interosseous muscle in the hand and anterior tibial muscle. SOD1 mutations were not identified in the genetic testing.

On admission, a presumptive diagnosis of familial ALS was made due to the patient's family history, the involvement of the upper and lower motor neurons in the brain stem (and upper and lower extremities), as well as a lack of sensory disturbance. However, the CSF neopterin concentration obtained on admission was elevated at 143.17 pmol/mL (normal concentrations ≤30 pmol/mL) (2) which was suggestive of an immune-mediated abnormality of the central nervous system. Therefore, testing for HTLV-I infection was conducted. The patient's serum and CSF anti-HTLV-I antibody titers were elevated (1:51,200 in serum and 1:128 in CSF). The HTLV-I proviral DNA load in the peripheral blood mononuclear cells (PBMCs) was high at 498 copies/10^4 cells [the mean±SD of HTLV-1 proviral load in asymptomatic HTLV-I carriers is 120±17 copies/10^4 PBMCs (3)]. We diagnosed this case as having HAM for the following reasons: 1) the titer of anti-HTLV-I antibody (1:128) in CSF was too high as a HTLV-I carrier with the other neurological disorders and 2) the 498 copies of HTLV-I proviral load was excessively high as a HTLV-I carrier. Matsuzaki et al. reported that ALS-like HAM patients with high HTLV-I proviral loads respond well to steroid therapy (4). Therefore, steroid therapy with intravenous infusions of methylprednisolone (1,000 mg/day) for 3 days was started and the CSF neopterin concentration rapidly fell to 50.33 pmol/mL after treatment. Subsequently, therapy with oral prednisolone was initiated at a dose of 15 mg daily. Although the dyslalia still persisted, it has improved moderately. The patient's grip strength (kg) improved from 12/13 (right/left hand) to 14/18. Her micturition frequency has reduced from approximately ten times daily to six times daily. Although amelioration of the gait disturbance has not been observed, the frequency of falls has decreased. After discharge, the dose of prednisolone was tapered. At a dose of 5 mg daily, micturition frequency increased and the CSF neopterin concentration rose to 194 pmol/mL. Hence, the dose of prednisolone was increased to 10 mg daily. Thereafter, the patient's symptoms remained stable without deterioration.

Discussion

There are several reports of HAM presenting with ALS-like symptoms as was seen in our case. In one case HAM was diagnosed on the basis of autopsy results; the subject was diagnosed as having ALS in life because of bulbar palsy and involvement of the lower and upper motor neurons in the extremities without sensory disturbance or bladder and rectal dysfunction. Several studies have reported HAM patients presenting with ALS-like features (4-9); these include a patient with bulbar palsy, systemic muscular atrophy and weakness, increased tendon reflexes of the extremities, and no sensory disturbance and a patient with bulbar palsy, systemic muscular atrophy and weakness, decreased vibratory sense in the lower legs, and impaired urination.

However, an autopsy was not performed in any of these patients. Autopsy reports on ALS-like HAM patients have described infiltration of inflammatory cells and dropout and degeneration of neural cells in the dorsal column, brain stem, cerebellum, and cerebrum in addition to the main lesions in the lateral column of the thoracic spinal cord (5, 10). Another autopsy report indicated that there were no Bunina bodies, which are unique to ALS (11).

There are two possibilities of the pathogenesis of this case: 1) HAM and ALS could have been coincidental and the inflammation process of HAM modified the ALS symptoms or 2) all of the ALS-like features were caused by HTLV-1-induced inflammation in the CNS. In the present case, the patient's symptoms began with dyslalia at approximately 40 years of age and she became unable to speak at 52 years of age. However, she was able to communicate by writing and could still walk, suggesting a slower rate of progression than that of ALS. Matsuzaki et al. reported that the average interval between onset of disease and the inability to walk is 5 years in patients with ALS-like HAM with a high HTLV-I proviral load (Table), indicating a slower rate of progression compared to typical ALS (4). Steroid therapy was not effective in ALS-like HAM patients with a low HTLV-I proviral load similar to that in asymptomatic HTLV-I carriers, whereas in ALS-like HAM patients with a high HTLV-I proviral load, steroid therapy was highly effective with efficacy almost equivalent to that seen in typical HAM patients (4, 12). The improved symptoms in our patient remained stable without deterioration by oral steroid therapy. On the basis of the high HTLV-I proviral load and the favorable response to steroid therapy, in addition to a slower progression of symptoms than that of ALS, our case was considered to be consistent with HAM presenting with ALS-like features. The measurement of neopterin and HTLV-I proviral load in HAM patients may be useful in differentiating HAM with ALS-like symptoms from ALS developing in HTLV-I carriers. Even in patients who have classical symptoms of ALS, the measurement of serum anti-HTLV-I antibody is of particular significance for differentiating HAM from ALS because half of the ALS-like HAM patients who receive steroid therapy show improvement in their symptoms.

The authors state that they have no Conflict of Interest (COI).

References

1. Osame M, Usuku K, Izumo S, et al. HTLV-I associated myelopathy, a new clinical entity. Lancet **1**: 1031-1032, 1986.
2. Nomoto M, Utatsu Y, Soejima Y, Osame M. Neopterin in cerebrospinal fluid: a useful marker for diagnosis of HTLV-I-associated myelopathy/tropical spastic paraparesis. Neurology **41**: 457, 1991.
3. Nagai M, Usuku K, Matsumoto W, et al. Analysis of HTLV-I proviral load in 202 HAM/TSP patients and 243 asymptomatic HTLV-I carriers: high proviral load strongly predisposes to HAM/TSP. J Neurovirol **4**: 586-593, 1998.
4. Matsuzaki T, Nakagawa M, Nagai M, et al. HTLV-I-associated myelopathy (HAM)/tropical spastic paraparesis (TSP) with amyotrophic lateral sclerosis-like manifestations. J Neurovirol **6**: 544-548, 2000.
5. Kuroda Y, Sugihara H. Autopsy report of HTLV-I-associated myelopathy presenting with ALS-like manifestations. J Neurol Sci Dec **106**: 199-205, 1991.
6. Arimura K, Nakagawa M, Izumo S, et al. HTLV-1-associated myelopathy (HAM) presenting with ALS-like feature. In: HTLV-1 and the Nervous System. Roman G, Vernant JC, Osame M, Eds. Alan R. Liss, New York, 1989: 367-370.
7. Vernant JC, Buisson G, Bellance R, François MA, Madkaud O, Zavaro O. Pseudo-amyotrophic lateral sclerosis, peripheral neuropathy and chronic polyradiculoneuritis in patients with HTLV-1-assosiated paraplegias. In: HTLV-1 and the Nervous System. Roman G, Vernant JC, Osame M, Eds. Alan R. Liss, New York, 1989: 361-365.
8. Evans BK, Gore I, Harrell LE, Arnold T, Oh SJ. HTLV-I-associated myelopathy and polymyositis in a US native. Neurology **39**: 1572-1575, 1989.
9. Silva MT, Leite AC, Alamy AH, Chimelli L, Andrada-Serpa MJ, Araújo AQ. ALS syndrome in HTLV-I infection. Neurology **65**: 1332-1333, 2005.
10. Iwasaki Y, Sawada K, Aiba I, et al. Widespread active inflammatory lesions in a case of HTLV-I-associated myelopathy lasting 29 years. Acta Neuropathol **108**: 546-551, 2004.
11. Souza A, Tanajura D, Toledo-Cornell C, Santos S, Carvalho EM. Immunopathogenesis and neurological manifestations associated to HTLV-I infection. Rev Soc Bras Med Trop **45**: 545-552, 2012.
12. Nagai M, Tsujii T, Iwaki H, Nishikawa N, Nomoto M. Cerebrospinal fluid neopterin, but not osteopontin, is a valuable biomarker for the treatment response in patients with HTLV-I-associated myelopathy. Intern Med **52**: 2203-2208, 2013.

ARTHRITIS & RHEUMATOLOGY
Vol. 67, No. 4, April 2015, pp 1096–1106
DOI 10.1002/art.39009

Direct Infection of Primary Salivary Gland Epithelial Cells by Human T Lymphotropic Virus Type I in Patients With Sjögren's Syndrome

Hideki Nakamura,[1] Yoshiko Takahashi,[1] Tomomi Yamamoto-Fukuda,[1] Yoshiro Horai,[1] Yoshikazu Nakashima,[1] Kazuhiko Arima,[1] Tatsufumi Nakamura,[2] Takehiko Koji,[1] and Atsushi Kawakami[1]

Objective. **To investigate whether human T lymphotropic virus type I (HTLV-I) directly infects salivary gland epithelial cells (SGECs) and induces the niche of the salivary glands in patients with Sjögren's syndrome (SS).**

Methods. **SGECs were cultured with the HTLV-I–producing CD4+ T cell line HCT-5 or with Jurkat cells. Antibody arrays, immunofluorescence analysis, and enzyme-linked immunosorbent assay (ELISA) were used to determine the profiles of inflammation-related molecules, and the profiles of apoptosis-related molecules were determined by antibody array and immunofluorescence analysis. The presence of HTLV-I–related molecules was assessed by immunofluorescence analysis and in situ polymerase chain reaction. Apoptosis of SGECs was evaluated by TUNEL staining.**

Results. **Among the SGECs, 7.8 ± 1.3% (mean ± SD) were positive for HTLV-I–related proteins after 96-hour coculture with HCT-5 cells. Nuclear NF-κB p65 was also detected in 10% of the SGECs. The presence of HTLV-I proviral DNA in SGECs after coculture with HCT-5 cells was detected by in situ polymerase chain reaction. After coculture of SGECs with HCT-5, the expression of cytokines and chemokines, including soluble intercellular adhesion molecule 1, RANTES, and interferon γ–induced protein 10 kd (IP-10/CXCL10) was increased in a time-dependent manner. The expression of proapoptotic molecules (e.g., cytochrome c and Fas) and antiapoptotic molecules (e.g., Bcl-2, Heme oxygenase 2, and Hsp27) was increased in the SGECs cocultured with HCT-5, showing that apoptosis of SGECs was not detected after coculture with HCT-5 or Jurkat cells.**

Conclusion. **HTLV-I is thought to infect SGECs and alter their cellular functions. These changes may induce the niche of SS and contribute to the development of SS in anti–HTLV-I antibody–positive individuals.**

Human T lymphotropic virus type I (HTLV-I) has been reported to be involved in the pathogenesis of primary Sjögren's syndrome (SS) in endemic areas, including Nagasaki City, Japan (1–3). The extremely high prevalence of SS among patients with HTLV-I–associated myelopathy (HAM) appears to confirm a strong relationship between HTLV-I infection and SS (4–6). A previous study by our group also revealed the clinical characteristics of anti–HTLV-I antibody–positive SS patients and showed that the labial salivary glands (LSGs) of such patients are not destructible compared with the LSGs of anti–HTLV-I antibody–negative patients with SS (7). In addition, the low prevalence of ectopic germinal centers (GCs) as well as the low expression of CXCL13 in infiltrating mononuclear cells in LSGs were shown to be immunohistologic characteristics of anti–HTLV-I antibody–positive patients with SS (8).

HTLV-I preferentially infects T cells, especially CD4+ T cells, and the observations described above indicate that the T cell lineage may primarily contribute

Supported in part by a grant from the Ministry of Health, Labor, and Welfare, Japan.

[1]Hideki Nakamura, MD, PhD, Yoshiko Takahashi, MD, Tomomi Yamamoto-Fukuda, MD, PhD, Yoshiro Horai, MD, Yoshikazu Nakashima, MD, Kazuhiko Arima, MD, PhD, Takehiko Koji, PhD, Atsushi Kawakami, MD, PhD: Nagasaki University Graduate School of Biomedical Sciences, Nagasaki, Japan; [2]Tatsufumi Nakamura, MD, PhD: Nagasaki International University, Nagasaki, Japan.

Address correspondence to Hideki Nakamura, MD, PhD, Unit of Translational Medicine, Department of Immunology and Rheumatology, Nagasaki University Graduate School of Biomedical Sciences, 1-7-1 Sakamoto, Nagasaki City, Nagasaki 852-8501, Japan. E-mail: nhideki@nagasaki-u.ac.jp.

Submitted for publication April 27, 2014; accepted in revised form December 19, 2014.

to the pathogenesis of anti–HTLV-I antibody–positive SS. However, cell types other than T cells, including the human retinal pigment epithelial cell line ARPE-19 (9), and human primary fibroblast-like synoviocytes (FLS) (10) were reported to be susceptible to HTLV-I infection. In ARPE-19 cells, the expression of intercellular adhesion molecule 1 (ICAM-1) is increased by HTLV-I, and the production of granulocyte–macrophage colony-stimulating factor (GM-CSF) from FLS is induced by HTLV-I.

These observations suggested that HTLV-I may infect cell lineages other than T cells in human salivary glands and may contribute to the development of SS. In this regard, ductal epithelial cells are considered candidate cells, because various cytokines, chemokines, and apoptosis-related molecules have been shown to be expressed in these cells (1). In addition, ductal epithelial cells attract T cells into the salivary glands of patients with SS through production of interferon-γ (IFNγ)–inducible 10-kd protein (IP-10; CXCL10) and monokine induced by IFNγ (CXCL9) (11).

In the current study, we investigated whether HTLV-I infects human primary salivary gland epithelial cells (SGECs) and modulates the production of functional molecules.

PATIENTS AND METHODS

Patients. Primary SGECs were obtained from the LSGs of 15 female patients with primary SS (mean ± SD age 53.2 ± 15.4 years). In all patients, SS was diagnosed according to the revised criteria proposed by the American–European Consensus Group (12), and anti–HTLV-I antibodies were absent, as measured by chemiluminescent enzyme immunoassay.

Antibodies and reagents. Mouse anti–HTLV-I antibodies (p19, p38, and Gag) were obtained from Chemicon, and mouse anti–NF-κB p65 antibody, mouse anti–cytochrome c antibody, mouse anti-Hsp27 antibody, and rabbit anti-Fas antibody were obtained from Santa Cruz Biotechnology. Mouse anti–heme oxygenase 2 (anti–HO-2) antibody was purchased from OriGene, and rabbit anti–ICAM-1 antibody, rabbit anti–growth-related oncogene (anti-GRO)/CXCL1 antibody, anti-CCL5/RANTES antibody, and rabbit anti–IP-10/CXCL10 antibody were purchased from LifeSpan Biosciences. Rabbit anti–interleukin-8 (anti–IL-8) antibody was purchased from ABgene. Secondary antibodies, including fluorescein isothiocyanate (FITC)–conjugated donkey anti-mouse IgG and tetramethylrhodamine isothiocyanate (TRITC)–conjugated donkey anti-rabbit IgG, were purchased from Jackson ImmunoResearch. Hoechst 33258 was purchased from Sigma. A Proteome Profiler Human Cytokine Array Kit, Panel A, and a Quantikine ELISA kit for soluble ICAM-1 (sICAM-1), CXCL10/IP-10, CCR5/RANTES, CXCL1/GROα, and CXCL8/IL-8 were purchased from R&D Systems. Cy3–dUTP was purchased from GE Healthcare. Monoclonal mouse anti-human CD4, anti-human CD8, anti-human CD20cy, mouse IgG1, and monoclonal rabbit anti-human cytokeratin 8/18 antibodies were purchased from Dako.

LSG biopsy and cell culture. Each patient underwent a lower lip salivary gland biopsy under local anesthesia. Some of the specimens were stained with hematoxylin to diagnose sialadenitis, and some were used for culture of SGECs in a defined keratinocyte–serum-free medium (SFM) (Invitrogen Life Technologies) supplemented with hydrocortisone (Sigma) and bovine pituitary extract (Kurabo). In all 15 patients, the diagnosis of SS was compatible with the Chisholm and Mason scale for histologic grading of LSG biopsy tissue (13).

For the coculture of SGECs with HTLV-I–producing T cells, HCT-5 cells (which are derived from the cerebrospinal fluid cells of patients with HAM [14]), were cultured with SGECs for the designated period of time in defined keratinocyte–SFM culture medium. As a control toward HCT-5, the non–HTLV-I–infected T cell line Jurkat was cultured in RPMI 1640 medium with 10% fetal bovine serum. For the experiments described below, HCT-5 or Jurkat cells were cocultured (2:1) with SGECs at the time when the cells were seeded. Briefly, the SGECs were seeded onto sterile coverslips for immunofluorescence analysis. Next, HCT-5 cells were added 24 hours after the SGECs attached to and grew on the coverslips. For immunofluorescence analysis, the cells were stringently washed with phosphate buffered saline (PBS) to remove any remaining HCT-5 cells. Informed consent for the use of LSG biopsy samples was obtained from all 9 patients at the commencement of the study. The study was conducted with the approval of the human ethics committee at Nagasaki University Hospital.

Immunofluorescence analysis. Immunofluorescence analyses were performed as previously described (15). Briefly, SGECs cultured on 12-mm^2 coverslips were fixed in PBS containing 4% paraformaldehyde (PFA) at 4°C, followed by immersion in methanol at −20°C for 10 minutes. After fixation, the SGECs were blocked in 5% normal horse serum in PBS and then incubated with the primary antibodies for 1 hour at room temperature, followed by incubation with FITC-conjugated and TRITC-conjugated secondary antibodies and Hoechst 33258, in the dark. The SGECs were then mounted in Vectashield mounting medium (Vector) and scanned with a fluorescence microscope (BIOREVO BZ-9000; Keyence). To measure the immunofluorescence of the HCT-5 cells, fixed cells were incubated with mouse primary monoclonal antibodies as cell surface markers, followed by FITC-conjugated secondary antibody and Hoechst 33258. Control experiments were performed to confirm the isotype specificity of the secondary antibodies. Immunostaining of HCT-5 cells was performed in the same manner as that described above for SGECs.

TUNEL staining. To investigate DNA double-strand breaks in SGECs, TUNEL staining was performed as described in a previous study by our group (16). After fixation, SGECs were incubated in 4% PFA at 4°C for 15 minutes, followed by immersion in PBS with 0.5% Tween 20 and 0.2% bovine serum albumin, using a MEBSTAIN Apoptosis Kit Direct (MBL). The SGECs were then incubated with a 50-μl terminal deoxynucleotidyl transferase solution at 37°C for 1 hour. The dUTP signal as detected by FITC was captured using a BIOREVO BZ-9000 fluorescence microscope (Keyence). TRAIL was used as a positive control to show induction of apoptosis (15).

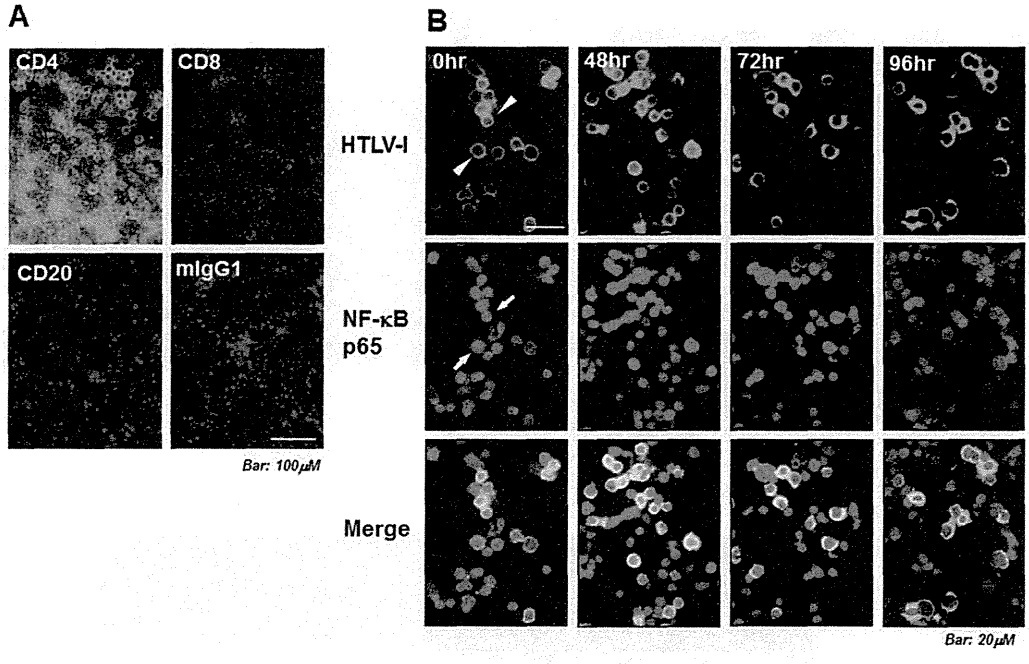

Figure 1. Characterization of the human T lymphotropic virus type I (HTLV-I)–infected HCT-5 T cell line. **A,** Phenotype of HCT-5 cells. After fixation in phosphate buffered saline containing 4% paraformaldehyde at 4°C followed by immersion in methanol at −20°C for 10 minutes, HCT-5 cells were incubated with primary antibodies (anti-CD4, anti-CD8, anti-CD20, and mouse IgG1 [mIgG1]) followed by fluorescein isothiocyanate (FITC)–conjugated secondary antibody and Hoechst 33258 (for counterstaining). **B,** Viability of HCT-5 cells. HCT-5 cells cultured for 0–96 hours in keratinocyte–serum-free medium were fixed and incubated with mouse anti–HTLV-I (p19, p28, and Gag) antibodies and rabbit anti–NF-κB p65 antibody and then incubated with FITC- and tetramethylrhodamine isothiocyanate–conjugated secondary antibodies and Hoechst 33258 (for counterstaining). **Arrowheads** indicate HTLV-I–related proteins including p19, p28, and Gag; **arrows** indicate NF-κB p65 translocation. Results are representative of 2 independent experiments with similar findings.

Cytokine detection in cocultured supernatant. A Proteome Profiler Cytokine Array system was used according to the manufacturer's instructions (R&D Systems). Briefly, after the membranes were blocked, diluted cocultured supernatant was incubated with a cocktail of biotinylated antibodies for 1 hour. The mixture of cytokines, chemokines, and antibodies was then incubated for 2 hours using this array system, combined with an immobilized antibody on the membrane. For the detection of cytokines and chemokines, chemiluminescent reagents were used after incubation with streptavidin–horseradish peroxidase (HRP).

Analysis of apoptosis in cocultured lysate. A Proteome Profiler Apoptosis Antibody Array system was used to analyze apoptosis pathways, according to the manufacturer's instructions (R&D Systems). Briefly, diluted cocultured cellular extracts were incubated on membranes for 2 hours after the membranes were blocked for 1 hour. After a 2-hour incubation, a cocktail of biotinylated antibodies was added to the membranes and incubated for 1 hour. Chemiluminescent reagents were then used after incubation with streptavidin–HRP for 30 minutes.

Cytokine and chemokine enzyme-linked immunosorbent assays (ELISAs). The levels of sICAM-1, CXCL10/IP-10, CCR5/RANTES, CXCL1/GROα, and CXCL8/IL-8 (all from R&D Systems) were measured by ELISA, according to the manufacturer's instructions. Briefly, the assigned volume of cell culture supernatant, standard, or control was added to an ELISA well and incubated for the indicated periods of time. After the wells were washed and decanted 3 times, each conjugate was added to a well and incubated for 1 hour at 4°C. After the washing process, substrate solution was added to each well and incubated for 15 minutes. After the addition of stop solution, optical density at 450 nm was measured.

In situ PCR of HTLV-I proviral DNA in cocultured SGECs. Initially, SGECs (alone or in coculture with HCT-5) were fixed in 0.5 ml Carnoy's fixative for 20 minutes at room temperature, followed by washing with 0.5 ml 70% ethanol for 15 minutes at room temperature on type I collagen–coated 12-mm^2 coverslips. After treatment with prewarmed protein kinase (1 μg/ml) at 37°C for 15 minutes and 3 washes with PBS, the SGECs were fixed with 4% PFA/PBS for 5 minutes and then were immersed in 50% formamide/2× saline–sodium citrate buffer at 4°C overnight. After being washed with deuterium-depleted water 3 times for 5 minutes each time, the cells were mixed with an amplification cocktail that consisted of a final concentration of 1× PCR buffer, 1 μg/ml forward primer (5′-CGGATACCCAGTCTACGTGT-3′), 1 μg/ml reverse primer (5′-GAGCCGATAACGCGTCC-3′) (17), 0.2 m*M* dNTP, 2.5 m*M* $MgCl_2$, 1 μ*M* Cy3–dUTP, and distilled water without DNA polymerase, and then boiled for 10 minutes.

Application of these primer sets was previously described

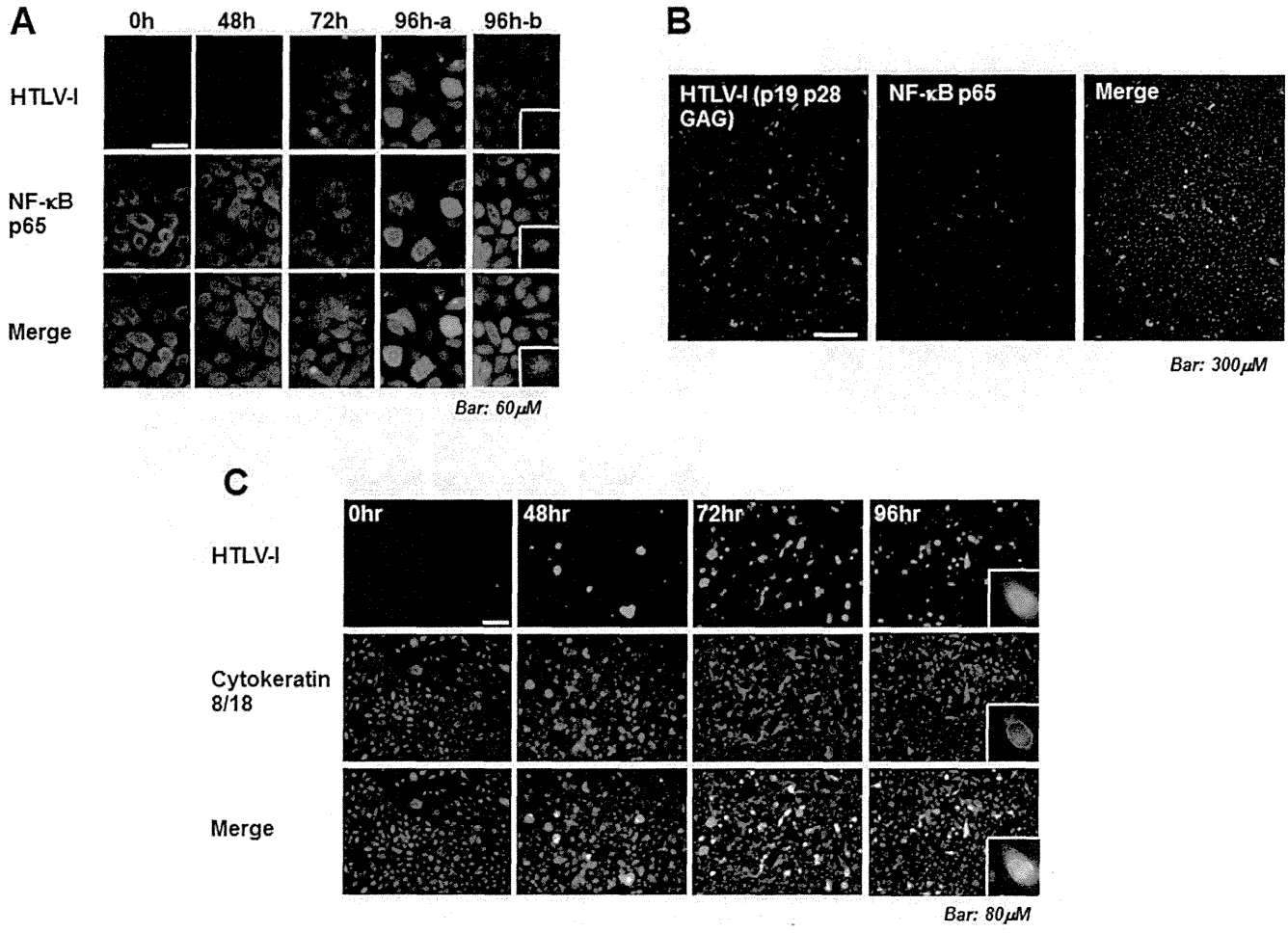

Figure 2. Detection of HTLV-I–related molecules in cocultured salivary gland epithelial cells (SGECs). **A,** Presence of HTLV-I proteins (p19, p28, and Gag), as determined by immunofluorescence analysis. SGECs cocultured for 0–96 hours were fixed in phosphate buffered saline containing 4% paraformaldehyde at 4°C followed by immersion in methanol at −20°C for 10 minutes. The SGECs were initially incubated with anti–HTLV-I antibody and NF-κB p65 followed by FITC- and tetramethylrhodamine isothiocyanate (TRITC)–conjugated secondary antibodies, respectively, and Hoechst 33258 for counterstaining. To contrast the increased expression of HTLV-I proteins without NF-κB translocation (96h-a), translocation of NF-κB is shown (96h-b). **B,** Low-magnification view of cocultured SGECs and HCT-5 cells at 96 hours, showing positive staining for HTLV-I in ~10% of SGECs. **C,** Frequency of HTLV-I–infected SGECs during 0–96-hour coculture, as determined by immunofluorescence analysis. SGECs were initially incubated with anti–HTLV-I antibody and anticytokeratin 8/18 antibody (to distinguish HTLV-I–infected SGECs from HCT-5 cells) followed by FITC- and TRITC-conjugated secondary antibodies, respectively, and Hoechst 33258 for counterstaining. In the merged view, yellow indicates HTLV-I–infected SGECs, and green indicates HCT-5 cells. Results are representative of 3 independent experiments. **Insets** in *A* and *C* show representative cells in each panel. See Figure 1 for other definitions.

in a study by Matsuoka et al, in which the positions of the forward and reverse primers were 7,358–7,377 and 7,516–7,494 of the HTLV-I pX region, respectively (17). After KAPA2G Fast DNA Polymerase complete amplification cocktail (Kapa Biosystems) was added to the SGECs and they were sealed with clear rubber covers, then the coverslips were placed in a thermocycler for in situ PCR (Hybaid). The details of the in situ PCR were as follows: each block was heated at 92°C for 3 minutes, 5 PCR cycles were performed (92°C for 1 minute, 47°C for 1 minute, and 70°C for 2 minutes), and the block was then held at 70°C for 5 minutes. The reacted coverslips were then washed 4 times with 2× saline–sodium citrate at 37°C for 15 minutes, followed by 2 washes with 0.5× saline–sodium citrate at 45°C for 15 minutes. After the coverslips were reacted with PBS once and covered with Vectashield mounting medium, SGECs were visualized using fluorochrome with a BIOREVO BZ-9000 fluorescence microscope.

Statistical analysis. Differences in ELISA results were analyzed using Student's *t*-test. *P* values less than 0.05 were considered significant.

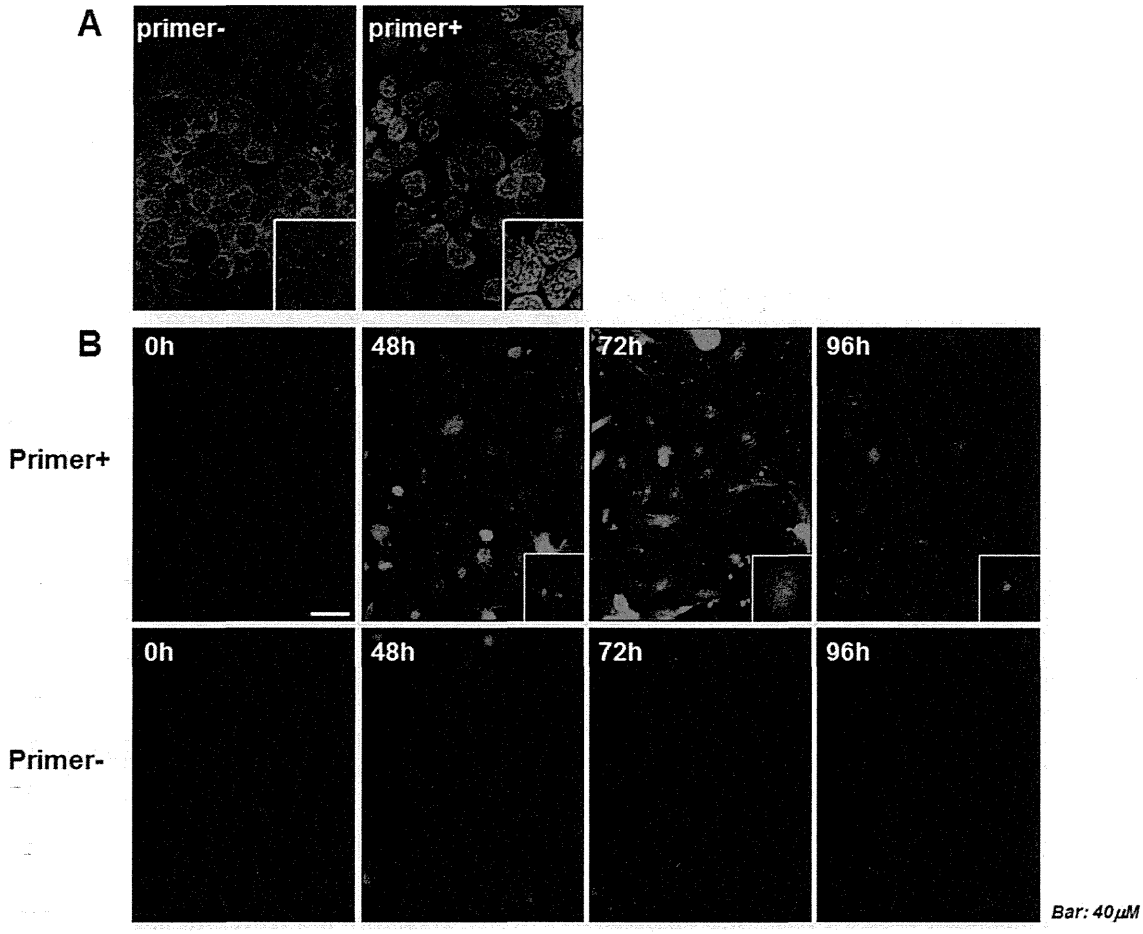

Figure 3. Detection of human T lymphotropic virus type I (HTLV-I) proviral DNA by in situ polymerase chain reaction (PCR). **A,** HTLV-I was detected in HCT-5 cells as a positive control. HCT-5 cells were treated with 1 μg/ml of protein kinase, and 5 cycles of in situ PCR were performed. Detected HTLV-I proviral DNA is shown as a granular pattern signal. **B,** Fixed salivary gland epithelial cells were treated with 1 μg/ml of protein kinase, and 5 cycles of in situ PCR were then performed in the presence or absence of primers for the HTLV-I pX region. Detected signal is indicated as the appearance of dots in the nucleus of salivary gland epithelial cells. Results are representative of 2 independent experiments with similar findings. **Insets** show representative cells in each panel.

RESULTS

Phenotype and viability of HCT-5 cells. The HCT-5 cells used for coculture with SGECs showed the CD4+ phenotype (Figure 1A), with no staining for CD8 or CD20. The HCT-5 cells cultured for 0–96 hours in keratinocyte–SFM were viable, with translocation of nuclear NF-κB into SGECs after coculture (Figure 1B).

Detection of HTLV-I–related proteins in SGECs during coculture. After coculture of SGECs and HCT-5 cells, immunofluorescence analysis showed clear signals for HTLV-I proteins p19, p28, and Gag at 72–96 hours (Figure 2A). At 96 hours, ~10% of the SGECs cocultured with HCT-5 cells showed HTLV-I–positive staining at low magnification (Figure 2B). Nuclear NF-κB p65 was also detected in 10% of the SGECs after coculture (Figures 2A and B). To distinguish HTLV-I–infected SGECs from HCT-5 cells, SGECs were stained with cytokeratin 8/18 antibodies (Figure 2C), which was reported to be one of markers for SGECs (18). In merged view (yellow signal), the mean ± SEM frequency of HTLV-I–infected SGECs was calculated as 7.8 ± 1.3%, and the remaining HCT-5 cells (green signal) were observed during coculture for 48–96 hours.

Detection of HTLV-I DNA in SGECs by in situ PCR. To clarify whether HTLV-I infected SGECs during coculture with HCT-5 cells and investigate the details, we determined HTLV-I DNA expression. As a positive control, HTLV-I proviral DNA was detected in HCT-5 cells (Figure 3A).

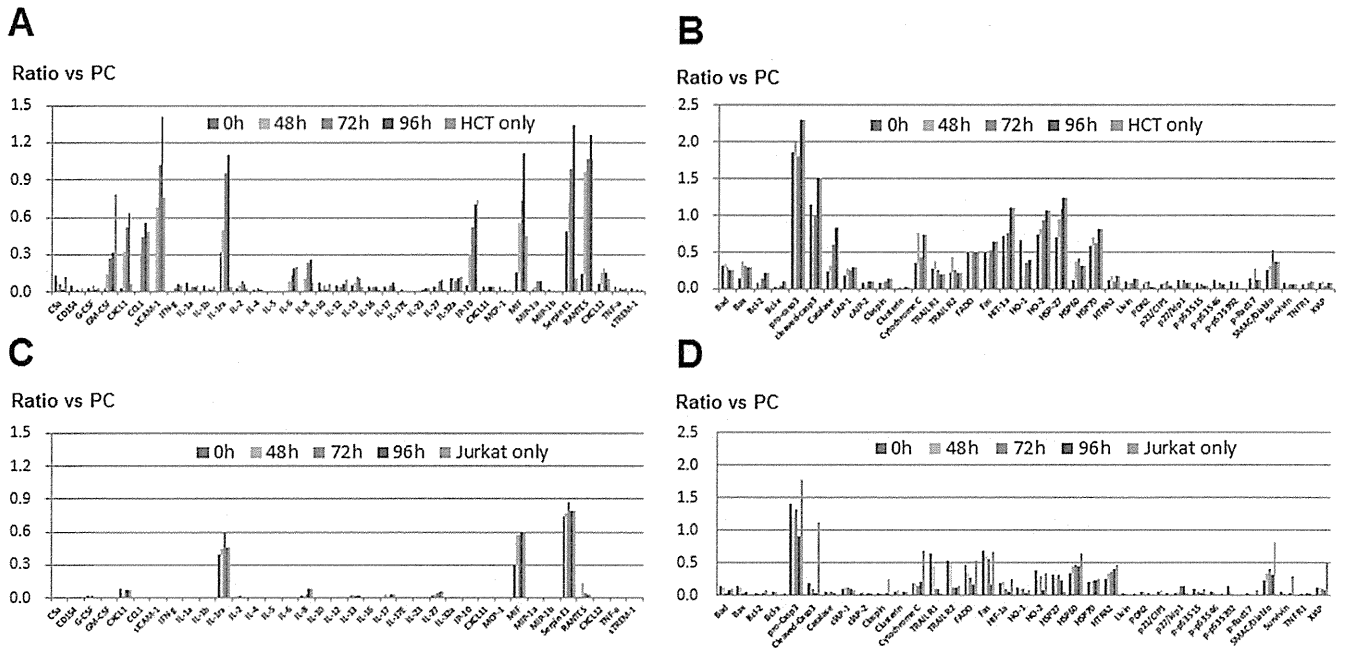

Figure 4. Expression of inflammation-related molecules and apoptosis-related molecules. **A** and **C,** Expression of inflammation-related molecules in supernatant of salivary gland epithelial cells (SGECs) cocultured with HCT-5 cells (**A**) or Jurkat cells (**C**). The semiquantitative concentrations of each molecule in culture medium (i.e., keratinocyte–serum-free medium) after coculture with HCT-5 cells or Jurkat cells is shown. "HCT-5 only" and Jurkat only" indicate the culture supernatant for HCT-5 cells and Jurkat cells, respectively. **B** and **D,** Expression of apoptosis-related molecules in lysate of SGECs cocultured with HCT-5 cells (**B**) or Jurkat cells (**D**). The semiquantitative concentration of each molecule in recovered SGEC lysate after coculture with HCT-5 cells or Jurkat cells is shown. Results are representative of 2 independent experiments with similar findings. PC = positive control.

During coculture, amplified HTLV-I DNA was observed in the nucleus of SGECs in the presence of primer at 48 hours of coculture with HCT-5 cells (Figure 3B). The strongest HTLV-I DNA signal was observed in the presence of primer at 72 hours of coculture.

Increased expression of inflammation-related molecules and apoptosis-related molecules in cocultured SGECs. As shown in Figure 4A, the expression of GM-CSF, CXCL1/GROα, CCL1, sICAM-1, IL-1 receptor antagonist (IL-1Ra), IL-6, IL-8, CXCL10/IP-10, macrophage migration inhibitory factor (MIF), serpin E1, and CCR5/RANTES in cocultured HCT-5/SGEC supernatant increased in a time-dependent manner. The results of apoptosis analysis using SGEC lysate cocultured with HCT-5 are shown in Figure 4B. The responses of proapoptotic molecules including procaspase 3, cytochrome c, and Fas in the lysate were slightly increased after coculture of SGECs with HCT-5 cells. The signals for antiapoptotic molecules including Bcl-2, HO-2, Hsp27, or second mitochondria-derived activator of caspases (SMAC)/Diablo were also up-regulated after coculture.

As shown in Figures 4C and D, the expression of IL-1Ra, MIF, and serpin E1 was increased after coculture of SGECs with Jurkat cells; however, the increase was not time dependent (Figure 4C). In contrast to the results of coculture of SGECs with HCT-5, expression of other molecules including GM-CSF, CXCL1/GROα, CCL1, sICAM-1, IL-6, IL-8, and CXCL10/IP-10 was not increased following coculture of SGECs with Jurkat cells. The results of the apoptosis analysis using SGEC lysate cocultured with Jurkat cells are shown in Figure 4D. Although expression of procaspase 3 and SMAC/Diablo was similar to that observed in HCT-5/SGEC coculture, expression of cytochrome c, Fas, Bcl-2, HO-2 and Hsp27 was not up-regulated after coculture of SGECs with Jurkat cells.

The data derived from analyses using a cytokine array system and an apoptosis antibody array system were confirmed by immunofluorescence analysis and ELISA. Immunofluorescence analysis showed increased cytoplasmic expression of ICAM-1, CXCL1, RANTES, IL-8, and IP-10 (Figure 5A), with augmentation of the signals for HTLV-I p19, p28, and Gag in SGECs after

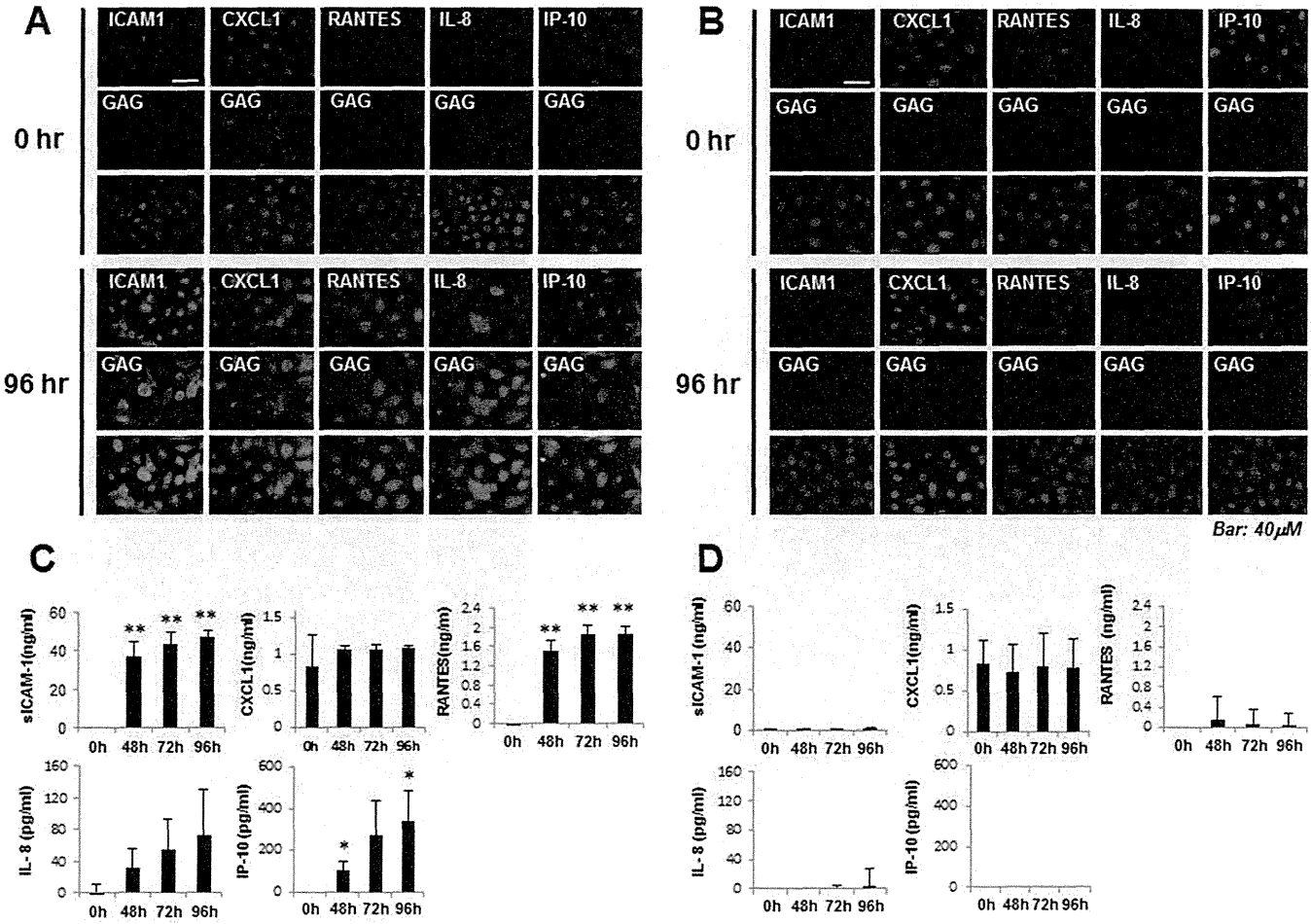

Figure 5. Increased expression of inflammation-related molecules in coculture supernatant, as confirmed by immunofluorescence analysis and enzyme-linked immunosorbent assay (ELISA). **A** and **B,** Expression of intercellular adhesion molecule 1 (ICAM-1), CXCL-1, RANTES, interleukin-8 (IL-8), and interferon-γ–inducible 10-kd protein (IP-10) in salivary gland epithelial cells (SGECs) cocultured with HCT-5 cells (**A**) or Jurkat cells (**B**), as determined by immunofluorescence analysis. The third rows in each panel show merged views. Yellow signal indicates coexpression of signal from top and middle rows. Results are representative of 2 independent experiments with similar findings. GAG = human T lymphotropic virus type I–related proteins p19, p28, and Gag. **C** and **D,** Concentrations of soluble ICAM-1 (sICAM-1), CXCL1/GROα, CCR5/RANTES, CXCL8/interleukin-8 (IL-8) and CXCL10/IP-10, in supernatant of SGECs cocultured with HCT-5 cells (**C**) or Jurket cells (**D**), as determined by ELISA. Values are the mean ± SD (n = 3 samples). * = $P < 0.05$; ** = $P < 0.01$ versus 0 hour, by Student's *t*-test.

96-hour coculture with HCT-5 cells. However, the expression of ICAM-1, CXCL1, RANTES, IL-8, and IP-10 was not increased when SGECs were cocultured with Jurkat cells (Figure 5B). Accordingly, significant increases in the expression of sICAM-1, RANTES, and IP-10 in the cocultured supernatant were confirmed by ELISA (Figure 5C). In SGEC/Jurkat cell coculture supernatant, however, no significant increase in sICAM-1, RANTES, and IP-10 expression was observed (Figure 5D). Furthermore, these molecules as well as IL-8 were scarcely detectable in SGEC/Jurkat cell coculture supernatant. The results of immunofluorescence analysis of apoptosis-related molecules also showed that the membranous expression of Fas on SGECs as well as the cytoplasmic expression of Bcl-2, cytochrome c, HO-2, and Hsp27 were up-regulated after 96-hour coculture with HCT-5 (Figure 6A). Compared with the results for HCT-5/SGEC coculture, no increase in apoptosis-related molecules was observed on SGECs cocultured with Jurkat cells (Figure 6B).

No detection of apoptosis of cocultured SGECs. We previously reported that cultured SGECs are committed to apoptosis by several stimuli (15,16). Because in the present study the expression of proapoptotic mole-

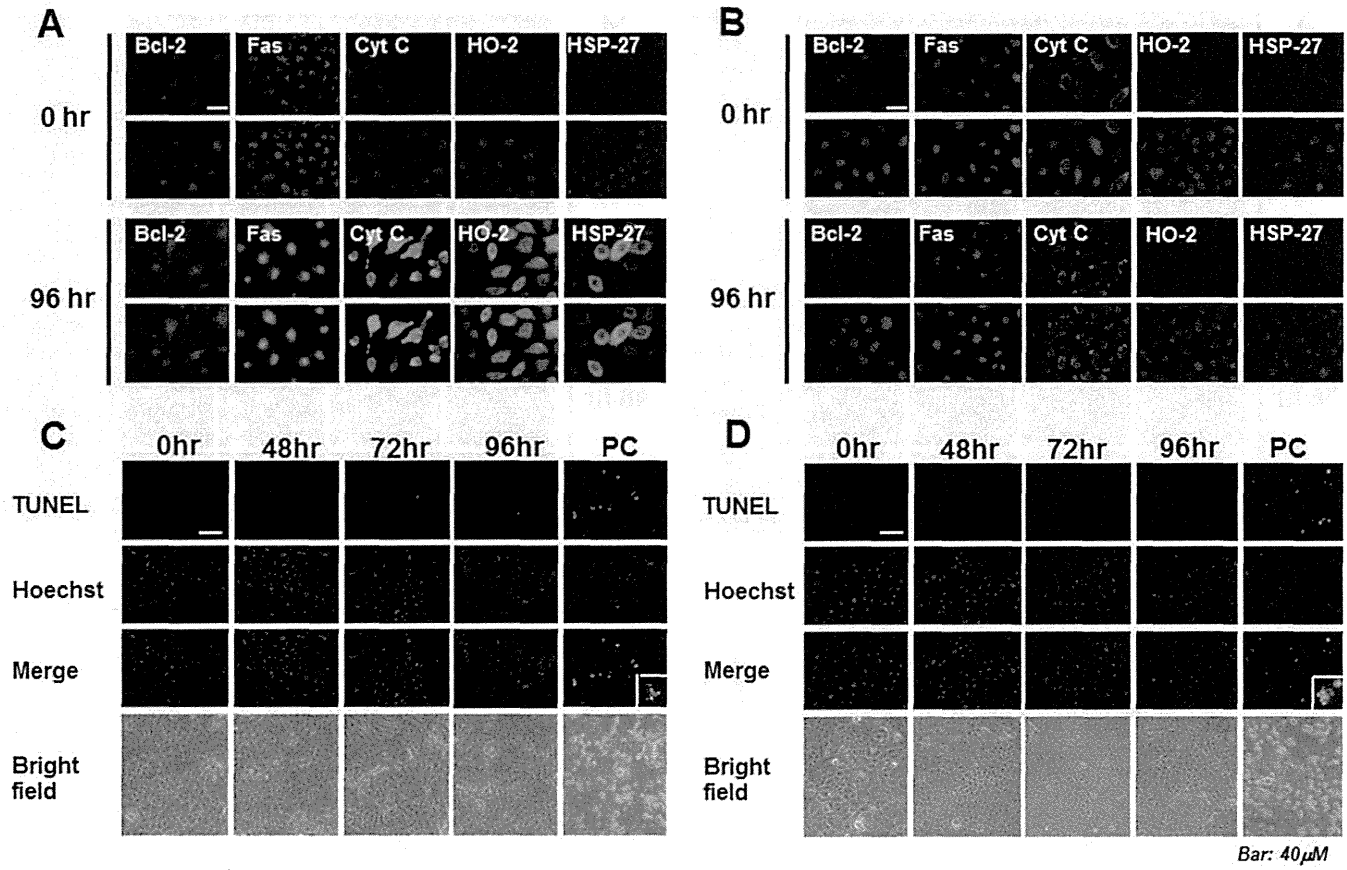

Figure 6. Expression of apoptosis-related molecules in cocultured salivary gland epithelial cells (SGECs). **A** and **B,** Expression of Bcl-2, Fas, cytochrome c (Cyt C), heme oxygenase 2 (HO-2), and Hsp27 in supernatant of SGECs cocultured with HCT-5 cells (**A**) or Jurkat cells (**B**), as determined by immunofluorescence analysis. **C** and **D,** Apoptosis of SGECs as evaluated by TUNEL staining. SGECs were cocultured with HCT-5 cells (**C**) or Jurkat cells (**D**) for 0–96 hours, followed by fixation in phosphate buffered saline containing 4% paraformaldehyde at 4°C and immersion in methanol at −20°C for 10 minutes, and were analyzed for TUNEL staining; Hoechst 33258 was used for nuclear staining. The fluorescein isothiocyanate–conjugated green signal indicates the presence of TUNEL-positive cells. As a positive control (PC), the SGECs were treated with TRAIL for 3 hours. Results are representative of 2 independent experiments with similar findings.

cules was increased by coculture with HCT-5 cells, it could be speculated that coculture with HCT-5 cells might induce apoptosis of SGECs. As we showed previously, the number of TUNEL-positive cells was clearly increased in SGECs stimulated with TRAIL (Figure 6C). In contrast, during 0–96-hour coculture, no TUNEL-positive staining was observed in SGECs cocultured with HCT-5 cells (Figure 6C). In addition, no obvious morphologic change was observed on brightfield views during coculture. Similarly, no TUNEL-positive staining was observed in SGECs during 0–96-hour coculture with Jurkat cells (Figure 6D).

DISCUSSION

With regard to the relationship between primary SS and retrovirus, Talal et al first reported that serum antibodies against human immunodeficiency virus 1 were detected in 30% of sera from patients with primary SS (19), and the presence of retroviral particles was observed in salivary gland tissue from patients with SS (20). Retroviral particles were also observed in the LSGs of patients with SS (21).

Regarding HTLV-I infection in patients with primary SS, Mariette et al reported the presence of the HTLV-I *tax* gene in the LSGs of patients with primary SS; however, the LSGs of patients with other inflammatory diseases also contained this gene, suggesting that the HTLV-I *tax* gene contributes to the development of chronic inflammatory diseases including primary SS (22,23). In addition, Green et al reported that HTLV-I Tax–transgenic mice exhibited exocrinopathy involving the salivary glands, and Tax

protein was detected in their salivary glands and muscle specimens (24).

A recent study showed that HTLV-I p19 or Tax protein was expressed in 42.4% of LSG samples from patients with SS, and the clinical characteristics of these SS patients (including low levels of complement and high lymphocyte counts) were identified (25). Considering the accumulating evidence of a relationship between HTLV-I and SS, we speculate that HTLV-I may directly infect SGECs, a major cellular constituent of the salivary glands, and change their characteristics to an inflammatory phenotype, triggering the development of SS.

In the present study, we observed for the first time that HTLV-I appears to infect SGECs, although the expression of HTLV-I–related protein was <10% among cocultured SGECs. The migration of HTLV-I into SGECs was suggested to induce functional alterations of SGECs, because some of the SGECs became positive for nuclear NF-κB p65, which is a transcription factor known to be activated by HTLV-I (26). Accordingly, the production of several inflammatory cytokines and chemokines increased during coculture of SGECs with HCT-5 cells in the current study. However, one or more pathways other than direct infection of SGECs by HTLV-I may be used, because a substantial population of SGECs showed no staining for HTLV-I–related proteins, HTLV-I proviral DNA, or nuclear NF-κB p65 after coculture. Autocrine or paracrine interactions of cytokines and chemokines might be involved in these processes, in which cytokines and chemokines induce the production reciprocally (27).

Alternatively, transcription factors or activators other than NF-κB p65, such as CREB/activating transcription factor and CREB-binding protein, which serves as a transcription activator, might be essential (28,29). Whether unique changes induced by HCT-5 are consequences attributable to direct infection of SGECs by HTLV-I or are an indirect effect of the molecules produced by neighboring activated cells (including HCT-5) is a crucial issue. In coculture, SGECs are spindle-shaped, and the intensity of Gag staining is not as strong as that in HCT-5 cells, suggesting that SGECs are distinguishable from HCT-5 cells. Some SGECs became double positive with Gag and inflammatory molecules in the coculture (Figure 5A). Because coculture of SGECs with the non–HTLV-I–infected T cell line Jurkat did not induce changes in the expression of functional molecules, cell-free HTLV-I virions might contribute to the changes in SGECs. Although no evidence of cell-free transmission of HTLV-I to any epithelial cells has been reported, HTLV-I virions have the potential to infect myeloid and plasmacytoid dendritic cells (DCs) (30). A previous study also showed that DC-SIGN plays an important role in cell-free HTLV-I infection of DCs (31). Further studies investigating cell-free infection of SGECs by HTLV-I virions are needed in the future.

In the current study, in addition to inflammatory cytokines and chemokines, both proapoptotic and antiapoptotic molecules were augmented in SGECs after coculture with HCT-5 cells compared with coculture with Jurkat cells. However, we should also note that the results of the apoptosis analysis might be influenced by the remaining HCT-5 cells during coculture. As shown in Figure 2C, HCT-5 cells attached to SGECs during coculture, and ~5% of HCT-5 cells still remained at 96 hours. It is possible that HCT-5 cells remained in coculture because these cells had migratory and adhesive capacity; we previously reported that CD4+ T cells derived from patients with HAM showed strong transmigrating activity (32).

The increased expression of these molecules may be induced via activation of transcription factors including NF-κB p65 or by the cytokines and chemokines produced by SGECs themselves. It has been demonstrated that the expression of both proapoptotic molecules and antiapoptotic molecules is regulated by the mechanisms described above (33,34). Increases in the expression of antiapoptotic molecules such as Bcl-2, HO-2, and Hsp27 might antagonize the apoptosis-inducing capacities of Fas and cytochrome c in SGECs, indicating that apoptosis does not occur in SGECs.

It is interesting to note that HTLV-I infection of SGECs induces the niche of SS, because the expression pattern of cytokines, chemokines, proapoptotic molecules, and antiapoptotic molecules of SGECs cocultured with HCT-5 cells in vitro resembles the pattern observed in vivo in the salivary glands of SS patients (35). However, it is debatable whether the present in vitro results truly reflect in vivo observations in patients with anti–HTLV-I antibody–positive SS. In this regard, Ohyama et al reported that HTLV-I proviral DNA was not present in either acinar cells or ductal epithelial cells in the LSGs of patients with HTLV-I antibody–positive SS but was observed in the infiltrating T lymphocytes, as demonstrated by in situ PCR (36).

It has become evident that CD4+ T cells infected by HTLV-I resemble FoxP3+ Treg cells (37). Regulatory T cells produce regulatory cytokines such as IL-10 and transforming growth factor β (38), which might affect the migration of HTLV-I into ductal epithelial cells in vivo. Further studies are necessary to clarify the

differences and similarities of the in vitro role of HTLV-I infection in patients with SS.

In summary, we have shown that direct infection of human primary SGECs by HTLV-I induces the niche of the salivary glands in patients with SS. Our clinical and histologic examinations also revealed the characteristics of anti–HTLV-I antibody–positive SS patients, including the low rate of ectopic GC formation in LSGs and parotid gland destruction (7,8). Although the exact pathways used by HTLV-I in SS remain unclear, this study is the first investigation in humans showing that HTLV-I infects SGECs and thus has an impact on the induction of SS.

ACKNOWLEDGMENT

We thank Ms Rie Yamashita for providing technical assistance.

AUTHOR CONTRIBUTIONS

All authors were involved in drafting the article or revising it critically for important intellectual content, and all authors approved the final version to be published. Dr. H. Nakamura had full access to all of the data in the study and takes responsibility for the integrity of the data and the accuracy of the data analysis.

Study conception and design. H. Nakamura.

Acquisition of data. H. Nakamura, Takahashi, Yamamoto-Fukuda, Horai.

Analysis and interpretation of data. H. Nakamura, Yamamoto-Fukuda, Nakashima, Arima, T. Nakamura, Koji, Kawakami.

REFERENCES

1. Nakamura H, Kawakami A, Eguchi K. Mechanisms of autoantibody production and the relationship between autoantibodies and the clinical manifestations in Sjögren's syndrome. Transl Res 2006;148:281–8.
2. Terada K, Katamine S, Eguchi K, Moriuchi R, Kita M, Shimada H, et al. Prevalence of serum and salivary antibodies to HTLV-1 in Sjögren's syndrome. Lancet 1994;22;344:1116–9.
3. Hida A, Imaizumi M, Sera N, Akahoshi M, Soda M, Maeda R, et al. Association of human T lymphotropic virus type I with Sjögren syndrome. Ann Rheum Dis 2010;69:2056–7.
4. Nakamura H, Eguchi K, Nakamura T, Mizokami A, Shirabe S, Kawakami A, et al. High prevalence of Sjögren's syndrome in patients with HTLV-I associated myelopathy. Ann Rheum Dis 1997;56:167–72.
5. Nakamura H, Kawakami A, Tominaga M, Hida A, Yamasaki S, Migita K, et al. Relationship between Sjögren's syndrome and human T-lymphotropic virus type I infection: follow-up study of 83 patients. J Lab Clin Med 2000;135:139–44.
6. Eguchi K, Matsuoka N, Ida H, Nakashima M, Sakai M, Sakito S, et al. Primary Sjögren's syndrome with antibodies to HTLV-I: clinical and laboratory features. Ann Rheum Dis 1992;51:769–76.
7. Nakamura H, Takagi Y, Kawakami A, Ida H, Nakamura T, Nakamura T, et al. HTLV-I infection results in resistance toward salivary gland destruction of Sjögren's syndrome. Clin Exp Rheumatol 2008;26:653–5.
8. Nakamura H, Kawakami A, Hayashi T, Nakamura T, Iwamoto N, Yamasaki S, et al. Low prevalence of ectopic germinal centre formation in patients with HTLV-I-associated Sjögren's syndrome. Rheumatology (Oxford) 2009;48:854–5.
9. Liu B, Li Z, Mahesh SP, Kurup SK, Giam CZ, Nussenblatt RB. HTLV-1 infection of human retinal pigment epithelial cells and inhibition of viral infection by an antibody to ICAM-1. Invest Ophthalmol Vis Sci 2006;47:1510–5.
10. Sakai M, Eguchi K, Terada K, Nakashima M, Yamashita I, Ida H, et al. Infection of human synovial cells by human T cell lymphotropic virus type I: proliferation and granulocyte/macrophage colony-stimulating factor production by synovial cells. J Clin Invest 1993;92:1957–66.
11. Ogawa N, Ping L, Zhenjun L, Takada Y, Sugai S. Involvement of the interferon-γ–induced T cell–attracting chemokines, interferon-γ–inducible 10-kd protein (CXCL10) and monokine induced by interferon-γ (CXCL9), in the salivary gland lesions of patients with Sjögren's syndrome. Arthritis Rheum 2002;46:2730–41.
12. Vitali C, Bombardieri S, Jonsson R, Moutsopoulos HM, Alexander EL, Carsons SE, et al, and the European Study Group on Classification Criteria for Sjögren's Syndrome. Classification criteria for Sjögren's syndrome: a revised version of the European criteria proposed by the American-European Consensus Group. Ann Rheum Dis 2002;61:554–8.
13. Chisholm DM, Mason DK. Labial salivary gland biopsy in Sjögren's disease. J Clin Pathol 1968;21:656–60.
14. Fukushima N, Nakamura T, Nishiura Y, Ida H, Aramaki T, Eguchi K. HTLV-I production based on activation of integrin/ligand signaling in HTLV-I-infected T cell lines derived from HAM/TSP patients. Intervirology 2008;51:123–9.
15. Nakamura H, Kawakami A, Iwamoto N, Ida H, Koji T, Eguchi K. Rapid and significant induction of TRAIL-mediated type II cells in apoptosis of primary salivary epithelial cells in primary Sjögren's syndrome. Apoptosis 2008;13:1322–30.
16. Nakamura H, Kawakami A, Ida H, Koji T, Eguchi K. Epidermal growth factor inhibits Fas-mediated apoptosis in salivary epithelial cells of patients with primary Sjögren's syndrome. Clin Exp Rheumatol 2007;25:831–7.
17. Matsuoka E, Takenouchi N, Hashimoto K, Kashio N, Moritoyo T, Higuchi I, et al. Perivascular T cells are infected with HTLV-I in the spinal cord lesions with HTLV-I-associated myelopathy/tropical spastic paraparesis: double staining of immunohistochemistry and polymerase chain reaction in situ hybridization. Acta Neuropathol 1998;96:340–6.
18. Dimitriou ID, Kapsogeorgou EK, Abu-Helu RF, Moutsopoulos HM, Manoussakis MN. Establishment of a convenient system for the long-term culture and study of non-neoplastic human salivary gland epithelial cells. Eur J Oral Sci 2002;110:21–30.
19. Talal N, Dauphinee MJ, Dang H, Alexander SS, Hart DJ, Garry RF. Detection of serum antibodies to retroviral proteins in patients with primary Sjögren's syndrome (autoimmune exocrinopathy). Arthritis Rheum 1990;33:774–81.
20. Garry RF, Fermin CD, Hart DJ, Alexander SS, Donehower LA, Luo-Zhang H. Detection of a human intracisternal A-type retroviral particle antigenically related to HIV. Science 1990;250: 1127–9.
21. Yamano S, Renard JN, Mizuno F, Narita Y, Uchida Y, Higashiyama H, et al. Retrovirus in salivary glands from patients with Sjögren's syndrome. J Clin Pathol 1997;50:223–30.
22. Mariette X, Agbalika F, Daniel MT, Bisson M, Lagrange P, Brouet JC, et al. Detection of human T lymphotropic virus type I tax gene in salivary gland epithelium from two patients with Sjögren's syndrome. Arthritis Rheum 1993;36:1423–8.
23. Mariette X, Agbalika F, Zucker-Franklin D, Clerc D, Janin A, Cherot P, et al. Detection of the tax gene of HTLV-I in labial salivary glands from patients with Sjögren's syndrome and other diseases of the oral cavity. Clin Exp Rheumatol 2000;18:341–7.
24. Green JE, Hinrichs SH, Vogel J, Jay G. Exocrinopathy resembling

Sjögren's syndrome in HTLV-1 tax transgenic mice. Nature 1989; 341:72–4.
25. Lee SJ, Lee JS, Shin MG, Tanaka Y, Park DJ, Kim TJ, et al. Detection of HTLV-1 in the labial salivary glands of patients with Sjögren's syndrome: a distinct clinical subgroup? J Rheumatol 2012;39:809–15.
26. Lindholm PF, Reid RL, Brady JN. Extracellular Tax_1 protein stimulates tumor necrosis factor-β and immunoglobulin κ light chain expression in lymphoid cells. J Virol 1992;66:1294–302.
27. Ospelt C, Neidhart M, Gay RE, Gay S. Synovial activation in rheumatoid arthritis. Front Biosci 2004;9:2323–34.
28. Zhao LJ, Giam CZ. Human T-cell lymphotropic virus type I (HTLV-I) transcriptional activator, Tax, enhances CREB binding to HTLV-I 21-base-pair repeats by protein-protein interaction. Proc Natl Acad Sci U S A 1992;89:7070–4.
29. Suzuki T, Fujisawa JI, Toita M, Yoshida M. The trans-activator Tax of human T-cell leukemia virus type 1 (HTLV-1) interacts with cAMP-responsive element (CRE) binding and CRE modulator proteins that bind to the 21-base-pair enhancer of HTLV-1. Proc Natl Acad Sci U S A 1993;90:610–4.
30. Jones KS, Petrow-Sadowski C, Huang YK, Bertolette DC, Ruscetti FW. Cell-free HTLV-1 infects dendritic cells leading to transmission and transformation of $CD4^+$ T cells. Nat Med 2008;14:429–36.
31. Jain P, Manuel SL, Khan ZK, Ahuja J, Quann K, Wigdahl B. DC-SIGN mediates cell-free infection and transmission of human T-cell lymphotropic virus type 1 by dendritic cells. J Virol 2009; 83:10908–21.
32. Furuya T, Nakamura T, Shirabe S, Nishiura Y, Tsujino A, Goto H, et al. Heightened transmigrating activity of CD4-positive T cells through reconstituted basement membrane in patients with human T-lymphotropic virus type I-associated myelopathy. Proc Assoc Am Physicians 1997;109:228–36.
33. Kulms D, Schwarz T. NF-κB and cytokines. Vitam Horm 2006;74: 283–300.
34. Liang Y, Zhou Y, Shen P. NF-κB and its regulation on the immune system. Cell Mol Immunol 2004;1:343–50.
35. Delaleu N, Jonsson MV, Appel S, Jonsson R. New concepts in the pathogenesis of Sjögren's syndrome. Rheum Dis Clin North Am 2008;34:833–45.
36. Ohyama Y, Nakamura S, Hara H, Shinohara M, Sasaki M, Ikebe-Hiroki A, et al. Accumulation of human T lymphotropic virus type I–infected T cells in the salivary glands of patients with human T lymphotropic virus type I–associated Sjögren's syndrome. Arthritis Rheum 1998;41:1972–8.
37. Toulza F, Nosaka K, Tanaka Y, Schioppa T, Balkwill F, Taylor GP, et al. Human T-lymphotropic virus type 1-induced CC chemokine ligand 22 maintains a high frequency of functional $FoxP3^+$ regulatory T cells. J Immunol 2010;185:183–9.
38. Suri-Payer E, Fritzsching B. Regulatory T cells in experimental autoimmune disease. Springer Semin Immunopathol 2006;28: 3–16.

Clinical & Experimental Neuroimmunology

Clinical and Experimental Neuroimmunology **5** (2014) 209–215

ORIGINAL ARTICLE

Intracellular cyclic adenosine monophosphate regulates the efficiency of intercellular transmission of human T-lymphotropic virus type I

Tatsufumi Nakamura,[1] Katsuya Satoh,[1] Hideki Nakamura[2] and Hironori Yamasaki[3]

[1]Department of Molecular Microbiology and Immunology, Nagasaki University, [2]Unit of Translational Medicine, Department of Immunology and Rheumatology, Graduate School of Biomedical Sciences, Nagasaki University, [3]Center for Health and Community Medicine, Nagasaki University, Nagasaki, Japan

Keywords
actin polymerization; cyclic adenosine monophosphate; human T-lymphotropic virus type I; human T-lymphotropic virus type I-associated myelopathy/tropical spastic paraparesis; vasodilator-stimulated phosphoprotein

Correspondence
Tatsufumi Nakamura, MD, Department of Molecular Microbiology and Immunology, Graduate School of Biomedical Sciences, Nagasaki University, 1-12-4 Sakamoto, Nagasaki 852-8523, Japan.
Tel: +81-95-819-7263
Fax: +81-95-849-7270
Email: tatsu@nagasaki-u.ac.jp

Received: 7 October 2013; revised: 17 November 2013; accepted: 28 December 2013.

Abstract

Objective To investigate the relationship between the intercellular transmission efficiency of human T-lymphotropic virus type I (HTLV-I) and the signaling involved in actin polymerization during cytoskeletal reorganization in a comparative study of HTLV-I-infected T-cell lines derived from an HTLV-I-associated myelopathy/tropical spastic paraparesis (HAM/TSP) patient or an HTLV-I carrier.

Methods HCT-5 and TL-Su cells derived from an HAM/TSP patient and an HTLV-I carrier, respectively, were used as HTLV-I-infected T-cell lines. After co-cultivation of each HTLV-I-infected T-cell line with H9/K30 *luc* reporter cells, the relative luc activities were calculated to analyze the efficiency of intercellular transmission of HTLV-I. The intracellular levels of cyclic adenosine monophosphate (cAMP) or cyclic guanosine monophosphate (cGMP) were measured in enzyme-linked immunoassays. The expression of phosphorylated vasodilator-stimulated phosphoprotein (p-VASP) was analyzed by western blotting.

Results Treatment of HCT-5 cells with latrunculin B, an inhibitor of actin polymerization, significantly suppressed the relative luc activity. Western blotting analysis of HCT-5 cells treated with the adenylyl cyclase activator forskolin showed upregulation of p-VASP, with a concomitant and significant increase in the intracellular cAMP concentration. Furthermore, the relative luc activity was significantly decreased. The intracellular cAMP, but not cGMP levels, were significantly lower in HCT-5 than in TL-Su. Vasodilator-stimulated phosphoprotein appeared less phosphorylated in HCT-5 than in TL-Su. The relative luc activity was significantly higher in HCT-5 than in TL-Su.

Conclusions The intracellular cAMP concentration regulates the efficiency of intercellular HTLV-I transmission under the control of p-VASP expression, suggesting the intercellular transmission potential of HTLV-I-infected T cells of HAM/TSP patients is enhanced by downregulated intracellular cAMP levels. (Clin. Exp. Neuroimmunol. doi: 10.1111/cen3.12097, February 2014)

Introduction

Human T-lymphotropic virus type I (HTLV-I) infects cells by intercellular transmission through the virological synapse, which is composed of integrin/ligand complexes, such as lymphocyte function antigen-1 (αLβ2)/intercellular adhesion molecule-1 (ICAM-1), and mediates cytoskeletal polarization.[1–3] Integrin/ligand signaling induces the activation of small GTPases, such as Rho, Rac and Cdc42, and subsequently regulates cytoskeletal reorganization including actin polymerization, cell polarity and reorientation of the microtubule-organizing center.[4–6] Therefore, it can be speculated that the status of